



Published in final edited form as:

J Cell Physiol. 2016 October ; 231(10): 2286–2302. doi:10.1002/jcp.25431.

AR-12 Inhibits Multiple Chaperones Concomitant With Stimulating Autophagosome Formation Collectively Preventing Virus Replication

LAURENCE BOOTH¹, JANE L. ROBERTS¹, HEATH ECROYD², SARAH R. TRITSCH³, SINA BAVARI³, ST. PATRICK REID³, STEFAN PRONIUK⁴, ALEXANDER ZUKIWSKI⁴, ABRAHAM JACOB⁵, CLAUDIA S. SEPÚLVEDA⁶, FEDERICO GIOVANNONI⁶, CYBELE C. GARCÍA⁶, ELSA DAMONTE⁶, JAVIER GONZÁLEZ-GALLEGO⁷, MARÍA J. TUÑÓN⁷, and PAUL DENT^{1,*}

¹Department of Biochemistry and Molecular Biology, Virginia Commonwealth University, Richmond, Virginia ²School of Biological Sciences and Illawarra Health and Medical Research Institute, University of Wollongong, New South Wales, Australia ³Molecular and Translational Science, United States Army Medical Research Institute of Infectious Diseases (USAMRIID), Fort Detrick, Frederick, Maryland ⁴Arno Therapeutics, Flemington, New Jersey ⁵Department of Otolaryngology, University of Arizona Ear Institute, Tucson, Arizona ⁶FCEN-UBA, Ciudad Universitaria, Pabellón 2 Piso 4, lab QB-17, Buenos Aires, Argentina ⁷Institute of Biomedicine and CIBEREhd, University of León, León, Spain

Abstract

We have recently demonstrated that AR-12 (OSU-03012) reduces the function and ATPase activities of multiple HSP90 and HSP70 family chaperones. Combined knock down of chaperones or AR-12 treatment acted to reduce the expression of virus receptors and essential glucosidase proteins. Combined knock down of chaperones or AR-12 treatment inactivated mTOR and elevated ATG13 S318 phosphorylation concomitant with inducing an endoplasmic reticulum stress response that in an eIF2 α —dependent fashion increased Beclin 1 and LC3 expression and autophagosome formation. Over-expression of chaperones prevented the reduction in receptor/glucosidase expression, mTOR inactivation, the ER stress response, and autophagosome formation. AR-12 reduced the reproduction of viruses including Mumps, Influenza, Measles, Junín, Rubella, HIV (wild type and protease resistant), and Ebola, an effect replicated by knock down of multiple chaperone proteins. AR-12—stimulated the co-localization of Influenza, EBV and HIV virus proteins with LC3 in autophagosomes and reduced viral protein association with the chaperones HSP90, HSP70, and GRP78. Knock down of Beclin 1 suppressed drug-induced

*Correspondence to: Paul Dent, PhD, 401 College Street, Massey Cancer Center, Box 980035, Department of Biochemistry and Molecular Biology, Virginia Commonwealth University, Richmond, VA 23298-0035. pdent@vcu.edu.

Authors' Contributions

Participated in research design: Dent, Ecroyd, Tunon, Gallego, Damonte, Proniuk, Zukiwski, Jacob, Reid. Conducted experiments: Booth, Roberts, Ecroyd, Sepulveda, Giovannoni, García, Tunon. Contributed new reagents/tools: n/a. Performed data analysis: Dent, Tunon, Gallego, Damonte, Tunon, Jacob. Contributed to manuscript writing: Dent, Ecroyd, Tunon, Gallego, Damonte.

Conflicts of interest: PD is the holder of the Universal Inc. Chair in Signal Transduction Research. Dr. Proniuk and Dr. Zukiwski are paid officers of Arno Therapeutics which owns the license to OSU-03012. The other authors have no conflicts of interest to report.

Supporting Information

Additional supporting information may be found in the online version of this article at the publisher's web-site.

autophagosome formation and reduced the anti-viral protection afforded by AR-12. In an animal model of hemorrhagic fever virus, a transient exposure of animals to low doses of AR-12 doubled animal survival from ~30% to ~60% and suppressed liver damage as measured by ATL, GGT and LDH release. Thus through inhibition of chaperone protein functions; reducing the production, stability and processing of viral proteins; and stimulating autophagosome formation/viral protein degradation, AR-12 acts as a broad-specificity anti-viral drug in vitro and in vivo. We argue future patient studies with AR-12 are warranted.

The drug OSU-03012 (AR12) was originally thought to act as an anti-cancer agent by inhibiting the enzyme PDK-1 within the PI3K pathway however it was subsequently shown that this compound was not primarily acting as a PDK-1 inhibitor, at least regarding the radio-sensitization of tumor cells (Zhu et al., 2004; Carón et al., 2005). Subsequently it was demonstrated that the primary mechanism by which AR-12 killed tumor cells was via the PKR-like endoplasmic reticulum kinase (PERK)—dependent induction of endoplasmic reticulum stress signaling and a toxic form of autophagy (Yacoub et al., 2006). Other studies then linked the effects of AR-12 on tumor cell biology to the regulation of chaperone proteins (Park et al., 2008). It was observed by western immunoblotting that AR-12 reduced the protein levels of HSP90 and GRP78 but stimulated HSP70 expression. Other groups independently confirmed this data regarding AR-12 and the induction of cytotoxic ER stress (Gao et al., 2008). As AR-12 down-regulates the PERK inhibitory chaperone GRP78, and as the induction of toxic autophagy was PERK dependent, additional studies further investigated the role of reduced GRP78 expression in the regulation of drug toxicity. AR-12 destabilized the GRP78 protein, reducing its half-life from >24 h to approximately 10 h (Booth et al., 2012). Over-expression of GRP78 prevented AR-12 induced PERK activation; autophagy induction, and tumor cell killing. Studies published in 2014 and 2015 further emphasized the importance of chaperones and particularly GRP78 in the biologic effects of OSU-03012. It was demonstrated that phosphodiesterase 5 inhibitors such as sildenafil synergized with OSU-03012 to kill a variety of tumor cells through enhanced PERK-dependent ER stress and autophagy, as well as through activation of the death receptor CD95 (Booth et al., 2014). Similar data were also obtained with the parent drug of OSU-03012, celecoxib, and also with the multi-kinase inhibitors sorafenib, regorafenib, and pazopanib (Booth et al., 2015a; Tavallai et al., 2015).

It is well-known that multiple chaperone proteins play essential roles in maintaining protein stability and cell signaling, and thus some chaperone proteins, for example, HSP90, have been the target for many developmental therapeutic chemists and also tumor cell biology researchers. In the field of virology, chaperone proteins, particularly HSPA5/GRP78/BiP have also been recognized as playing essential roles in the life cycles of both DNA and RNA viruses (Roux, 1990; Earl et al., 1991; Anderson et al., 1992; Hogue and Nayak, 1992; Xu et al., 1998; Mirazimi and Svensson, 2000; Bolt, 2001; Dimcheff et al., 2004; Goodwin et al., 2011; Dabo and Meurs, 2012; Rathore et al., 2013). Using OSU-03012 or the multi-kinase inhibitors sorafenib (Nexavar) and pazopanib (Votrient) it was determined, using in situ immunofluorescence techniques, that the expression of multiple chaperones was apparently rapidly reduced following drug treatment (Booth et al., 2015b; Roberts et al., 2015; Booth et al., 2016a). In these studies, parallel virology based assays determined that OSU-03012

exhibited anti-viral properties against a wide range of DNA and RNA viruses, and using molecular tools it was shown that the down-regulation of GRP78 was an essential property of OSU-03012 in preventing virus reproduction. Contemporaneously with the publication of these studies, other research groups were demonstrating that the expression of GRP78 was essential for Ebola virus reproduction in vitro with knock down of GRP78 protecting mice from Ebola virus, and that OSU-03012 prevented the replication of hemorrhagic fever viruses, including Ebola and Marburg (Reid et al., 2014; Mohr et al., 2015).

Very recently, proteomic studies using the OSU-03012 drug as bait were published (Booth et al., 2016a). Multiple chaperone and chaperone-associated proteins were shown to interact with the drug including: GRP75, HSP75, BAG2; HSP27; ULK-1; and thioredoxin. OSU-03012 altered the subcellular distribution of chaperone proteins and inhibited chaperone ATPase activity; inhibited chaperone—client interactions; and docked in silico with the ATPase domains of HSP90 and of HSP70. OSU-03012 combined with sildenafil in a GRP78 plus HSP27—dependent fashion to profoundly activate an eIF2 α /ATF4/CHOP/Beclin 1 pathway in parallel with inactivating mTOR and increasing ATG13 phosphorylation, collectively resulting in formation of punctate toxic autophagosomes. Over-expression of (GRP78 and HSP27) prevented OSU-03012—induced activation of ER stress signaling; maintained mTOR activity; and maintained cell survival (Booth et al., 2016a).

The virology focused studies in this manuscript were initiated to determine whether OSU-03012 altered virus replication and discovered that HSP90, HSP70, GRP78 and the small chaperone HSP27 are key OSU-03012 targets in terms of altering viral cell biology. AR-12 prolonged animal survival in a hemorrhagic fever virus animal model system. As AR-12 has already undergone phase I evaluation in heavily pre-treated cancer patients, our present data argue for patient based antiviral clinical studies.

Materials and Methods

Materials

OSU-03012, sildenafil, regorafenib, pazopanib, sorafenib tosylate were purchased from Selleckchem (Houston, TX). OSU-03012 (AR-12) and AR-13 were also kindly provided by Arno Therapeutics (Flemington NJ). Trypsin-EDTA, DMEM, RPMI, penicillin-streptomycin were purchased from GIBCOBRL (GIBCOBRL Life Technologies, Grand Island, NY). Cells were purchased from the ATCC and were not further validated beyond that claimed by ATCC. Cells were re-purchased every ~6 months. Primary human GBM cells, developed by Dr. C.D. James when at the Mayo Clinic (Rochester, MN) has been described previously (Yacoub et al., 2006; Park et al., 2008; Booth et al., 2016a). ADOR non-small cell lung cancer cells are personal a donation from the patient to the Dent laboratory. The plasmid to express GRP78/BiP/HSPA5 was kindly provided to the Dent laboratory by Dr. A.S. Lee (University of Southern California Los Angeles, CA). The plasmids to express HSP27, eIF2 α S51A, kinase inactive PERK and all others listed in this manuscript were purchased from Addgene (Cambridge, MA). Mumps, Measles, Rubella, Coxsackievirus B4, and Influenza viruses were purchased from Zeptomatrix (Buffalo, NY). Commercially available validated short hairpin RNA molecules to knock down RNA/protein

levels were from Qiagen (Valencia, CA) or were supplied by collaborators ([_S1_Reference5Booth et al., 2015a,b, 2016a,b,c](#); [Roberts et al., 2015](#); [Tavallai et al., 2015](#)).

Methods

Culture and in vitro exposure of cells to drugs.—All cell lines were cultured at 37°C (5% [v/v CO₂] in vitro using RPMI supplemented with dialyzed 5% [v/v] fetal calf serum and 10% [v/v] non-essential amino acids). For short term cell killing assays, immunoblotting studies, cells were plated in triplicate at a density of 3×10^3 per cm² ($\sim 2 \times 10^5$ cells per well of a 12 well plate) and 24 h after plating treated with various drugs, as indicated. In vitro drug treatments were from 100mM stock solutions of each drug and the maximal concentration of Vehicle (DMSO) in media was 0.02% (v/v). Studies were performed 2–3 times each and representative images presented, that is, cell death studies use multiple images from multiple independent treatments to achieve a percentage cell death value, where included (\pm SEM). Cells were not cultured in reduced serum media during any study in this manuscript.

Detection of cell viability, protein expression, and protein phosphorylation by immuno-fluorescence using a Hermes WiScan machine.—<http://www.idea-bio.com/>, cells (4×10^3) are plated into each well of a 96 well plate, and cells permitted to attach and grow for the next 18h. Based on the experiment, after 18h, cells are then either genetically manipulated, or are treated with drugs. For genetic manipulation, cells are transfected with plasmids or siRNA molecules and incubated for an additional 24 h. Cells are treated with vehicle control or with drugs at the indicated final concentrations, alone or in combination. Cells are then isolated for processing at various times following drug exposure. The 96 well plate is centrifuged/cyto-spun to associate dead cells (for live-dead assays) with the base of each well. For live dead assays, after centrifugation, the media is removed and cells treated with live-dead reagent (Thermo Fisher Scientific, Waltham MA) and after 10 min this is removed and the cells in each well are visualized in the Hermes instrument at 10 \times magnification. Green cells = viable; yellow/red cells = dying/dead. The numbers of viable and dead cells were counted manually from three images taken from each well combined with data from another two wells of separately treated cells (i.e., the data is the mean cell dead from nine data points from three separate exposures). For immuno-fluorescence studies, after centrifugation, the media is removed and cells are fixed in place and permeabilized using ice cold PBS containing 0.4% paraformaldehyde and 0.5% Triton X-100. After 30 min the cells are washed three times with ice cold PBS and cells are pre-blocked with rat serum for 3 h. Cells are then incubated with a primary antibody to detect the expression/phosphorylation of a protein (usually at 1:100 dilution from a commercial vendor) overnight at 37°C. Cells are washed three times with PBS followed by application of the secondary antibody containing an associated fluorescent red or green chemical tag. After 3 h of incubation the antibody is removed and the cells washed again. The cells are visualized at either 10 \times or 60 \times in the Hermes machine for imaging assessments. All immunofluorescent images for each individual protein/phospho-protein are taken using the identical machine settings so that the levels of signal in each image can be directly compared to the level of signal in the cells treated with drugs. Similarly, for presentation, the enhancement of image brightness/contrast using PhotoShop CS6 is simultaneously

performed for each individual set of protein/phospho-protein to permit direct comparison of the image intensity between treatments. Antibodies used include: HSP90 (E289) (Cell Signaling); HSP90 (#2928) (Abcam); HSP90 (ab195575) Abcam; HSP90 3G3 (13495) (Abcam); GRP78 (50b12) (31772) (Cell Signaling); GRP78 (ab191023) Abcam; GRP78 (ab103336) Abcam; GRP78 (N-20) (sc-1050) Santa Cruz; HSP27 (G31) (2402P) (Cell Signaling); HSP27 (EP1724Y) (ab62339) Abcam; HSP27 (H-77) (sc-9012) Santa Cruz; HSP27 (LS-C31836) Lifespan science Corp.

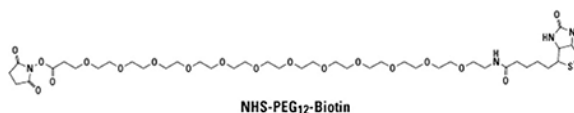
Immuno-histochemistry of tissues.—Athymic mice were treated by oral gavage with vehicle (cremophore); OSU-03012 (50 mg/kg) + sildenafil (10 mg/kg) for 14 days QD. Animals were sacrificed after 5 days (immuno-histochemistry) or 14 days (H&E staining) and normal tissue/organs obtained. Organs were fixed and 10 mm sections taken, de-parafinized and H&E stained. Color images were taken at 10× magnification (special thanks to Dr. Steven Grant, VCU, Department of Hematology/Oncology).

Rabbit hemorrhagic fever virus studies.—Nine-week-old New Zealand white rabbits were kept in the animal facility of the University of Leon. The rabbits were kept in a climatized room at 21°C, with a 12 h light cycle. They were given a standard dry rabbit food and water *ad libidum*. For animal survival studies, 14 animals were injected intramuscularly with 2×10^4 hemagglutination units of RHDV isolate Ast/89 (Tuñón et al., 2003). Seven were treated with vehicle control and seven of them were treated with OSU-03012 (AR-12) (25 mg/kg) at time = 0, 12, 24, and 36 h post infection. Animal survival was monitored twice daily.

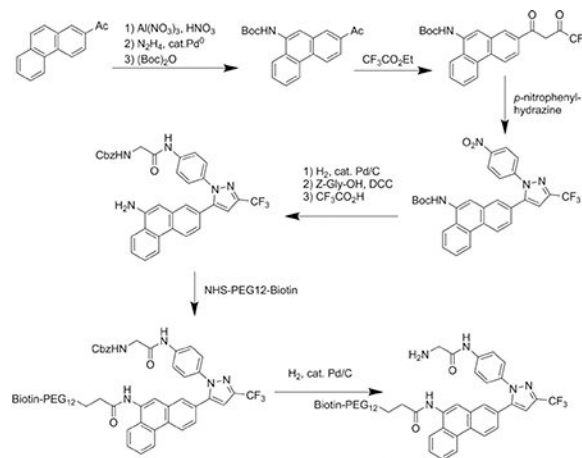
Proteomic/mass spectrometry procedures

Preparation of biotin-AR-12.—The strategy used to covalently link biotin to AR-12 exploited structure-activity relationships established by the Chen laboratory. Briefly, a biotin-linker arm conjugate (NHS-PEG12-biotin) was added to a region of the compound that was not associated with biological activity; its relatively long length was selected to minimize potential interference with the compound's active sites.

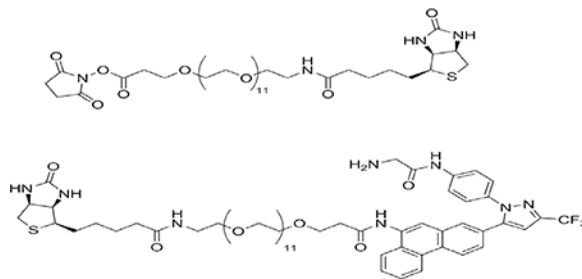
The linker arm has this structure:



The synthetic scheme is:



This scheme yields the following final biotin-AR-12 conjugate:



Sample preparation, SDS-PAGE, and tandem mass spectrometry analysis

Cultured SKBR3 HER2+ human mammary carcinoma cells were extracted after 24 h in serum free medium with ice cold buffer containing non-ionic detergent (Triton X100), protease and phosphatase inhibitors. Lysates were cleared of insoluble material by centrifugation. Supernatants were “pre-cleared” of molecules that bind non-specifically to streptavidin (SA) coated beads by incubating with SA-beads for 30 min at 4°C and subsequently removing the beads by centrifugation. Supernatant samples resulting from this step were then incubated with biotin-AR-12 in the presence or absence of excess AR-12 for 2 h at 4°C. SA-beads were then added for an additional 2 h at 4°C before capture by centrifugation, repeated washing with non-ionic detergent buffer and extraction with boiling Laemmli SDS-PAGE sample buffer. Samples were subjected to SDS-PAGE and bands were visualized using Ponceau S. Bands present in the biotin-AR-12 samples that were not found in the samples incubated with excess unlabeled AR-12 were excised from the gel, rinsed to remove Ponceau S and digested with trypsin. Eluted tryptic peptides were separated by nanotrap- and C18-column HPLC coupled to online analysis by tandem mass spectrometry (nLC-ESI-MS/MS) on an ion trap mass spectrometer equipped with a nanospray ion source using conventional techniques (Laboratory of Proteomic and Analytical Technologies, Frederick National Laboratory for Cancer Research, National Cancer Institute, Frederick, MD). The resulting MS/MS spectra were searched against the human IPI database to derive probable peptide amino acid sequence, protein/gene identities, and statistical confidence values (<http://blast.ncbi.nlm.nih.gov/Blast.cgi>).

Gel filtration of HeLa cell lysates.—HeLa cells were grown in 25 cm² flasks were exposed to AR-12 or sorafenib (both, 5 μM) or DMSO control for 20 min. Media was removed and cells washed with PBS containing 5 μM of drug (or equivalent volume of DMSO) two times. Cells were lysed with 1% Triton X-100 in PBS containing protease and phosphatase inhibitors (Pierce) and 5 μM of drug or equivalent volume of DMSO as a control. Samples were vortexed and then incubated at 4°C for 30 min on ice. Samples were centrifuged (20,000g, 20 min, 4°C) and supernatants collected and stored at 4°C until they were subjected to gel filtration. A Superdex 10/300 column (GE Healthcare) was pre-equilibrated with buffer (PBS) containing 5 μM drug or equivalent volume of DMSO at 0.5 ml/min. 200 μg of total protein was loaded onto the column (100 μl of sample) and proteins eluted with buffer at 0.5 ml/min. Fractions of 1 ml were collected as they eluted from the column. Those fractions containing protein (8–23) were collected and initially stored on ice. To each fraction, 250 μl of ice-cold trichloroacetic acid was added to a final concentration of 10% (w/v) to precipitate the proteins; each fraction was mixed vigorously and then incubated on ice overnight. Samples were then centrifuged (20,000g, 20 min, 4°C), the supernatant discarded and the protein pellet washed twice with cold acetone followed each time by additional centrifugations. Samples were then left to air-dry prior to SDS-PAGE and immunoblotting.

Transfection of cells with siRNA or with plasmids

For plasmids.—Cells were plated as described above and 24 h after plating, transfected. For mouse embryonic fibroblasts (2–5 μg) or other cell types (0.5 μg) plasmids expressing a specific mRNA (or siRNA) or appropriate vector control plasmid DNA was diluted in 50 μl serum-free and antibiotic-free medium (1 portion for each sample). Concurrently, 2 μl Lipofectamine 2000 (Invitrogen), was diluted into 50 μl of serum-free and antibiotic-free medium (1 portion for each sample). Diluted DNA was added to the diluted Lipofectamine 2000 for each sample and incubated at room temperature for 30 min. This mixture was added to each well/dish of cells containing 200 μl serum-free and antibiotic-free medium for a total volume of 300 μl, and the cells were incubated for 4 h at 37°C. An equal volume of 2× medium was then added to each well. Cells were incubated for 48 h, then treated with drugs.

Transfection for siRNA.—Cells were plated in 60 mm dishes from a fresh culture growing in log phase as described above, and 24 h after plating transfected. Prior to transfection, the medium was aspirated and 1 ml serum-free medium was added to each plate. For transfection, 10 nM of the annealed siRNA, the positive sense control double stranded siRNA targeting GAPDH or the negative control (a “scrambled” sequence with no significant homology to any known gene sequences from mouse, rat or human cell lines) were used. Ten nanomolars siRNA (scrambled or experimental) was diluted in serum-free media. Four microliters HiPerfect (Qiagen) was added to this mixture and the solution was mixed by pipetting up and down several times. This solution was incubated at room temp for 10 min, then added drop-wise to each dish. The medium in each dish was swirled gently to mix, then incubated at 37°C for 2 h. One microliter of 10% (v/v) serum-containing medium was added to each plate, and cells were incubated at 37°C for 48 h before re-plating (50 ×

10³ cells each) onto 12-well plates. Cells were allowed to attach overnight, then treated with drugs (0–24 h).

Methods for HIV/AR12 viral replication studies.—Arno Therapeutics compound AR-12 was supplied by the company as a dry powder to Southern Research and the stock was stored at 4°C until the day of the assays. The compound stock solution was used to generate working drug dilutions used in the assays on each day of assay setup. Working solutions were made fresh for each experiment and were not stored for re-use in subsequent experiments performed on different days. The compounds were evaluated in the assays using a 10 µM (10,000 nM) high-test concentration with eight additional serial 1:2 dilutions (concentration range = 39.1 nM to 10 µM). Similarly, zidovudine (AZT; Nucleoside Reverse Transcriptase Inhibitor; NRTI) was included as a positive control antiviral compound using half-log dilutions and a concentration range from 100 pM to 1.0 µM (1,000 nM). Various additional controls were also included for assays depending on the resistance profile of the viruses. Nevirapine (Non-Nucleoside Reverse Transcriptase Inhibitor; NNRTI) and ritonavir (Protease Inhibitor; PI) were tested using a concentration range from 1.0 nM to 10 µM (10,000 nM). Delavirdine (NNRTI) and T-20 (Fusion Inhibitor) were tested using a concentration range from 200 pM to 2.0 µM (2,000 nM). Elvitegravir (Integrase Inhibitor; INI) was tested using a concentration range from 100 pM to 1.0 µM (1,000 nM). Finally, raltegravir (INI) was tested using a concentration range from 10 pM to 100 nM. These studies were performed under DAIDS/ NIAID contract N01-A1–14000101; Roger Miller, Project Officer.

Efficacy evaluation in human peripheral blood mononuclear cells (PBMCs).—Six HIV-I isolates were selected for use. These viruses were chosen to include various drug resistant HIV-I isolates to evaluate potential cross-resistance to AR-12. Unless otherwise noted, these virus isolates were obtained from the NIAID AIDS Research and Reference Reagent Program. Virus isolate 1022–48 was obtained from Dr. William A Schief of Merck Research Laboratories. MDR769 and MDR807 were obtained from Dr. Thomas C. Merigan of Stanford University. The following table lists additional available information for each of the viruses.

Reverse transcriptase activity assay.—A microtiter plate-based reverse transcriptase (RT) reaction was utilized (Buckheit and Swanstrom, 1991). Tritiated thymidine triphosphate (3H-TTP, 80 Ci/mmol, PerkinElmer) was received in 1:1 dH₂O:Ethanol at 1 mCi/ml. Poly rA:oligo dT template:primer (GE HealthCare) was prepared as a stock solution by combining 150 µl poly rA (20 mg/ml) with 0.5 ml oligo dT (20 U/ml) and 5.35 ml sterile dH₂O followed by aliquoting (1.0 ml) and storage at –20°C. The RT reaction buffer was prepared fresh on a daily basis and consisted of 125 µl 1.0 M EGTA, 125 µl dH₂O, 125 µl 20% Triton X100, 50 µl 1.0 M Tris (pH 7.4), 50 µl 1.0 M DTT, and 40 µl 1.0 M MgCl₂. The final reaction mixture was prepared by combining 1 part 3H-TTP, 4 parts dH₂O, 2.5 parts poly rA:oligo dT stock and 2.5 parts reaction buffer. Ten microliters of this reaction mixture was placed in a round bottom microtiter plate and 15 µl of virus-containing supernatant was added and mixed. The plate was incubated at 37°C for 60 min. Following incubation, the reaction volume was spotted onto DE81 filter-mats (Wallac), washed five

times for 5 min each in a 5% sodium phosphate buffer or 2× SSC (Life Technologies), two times for 1 min each in distilled water, two times for 1 min each in 70% ethanol, and then dried. Incorporated radioactivity (counts per minute, CPM) was quantified using standard liquid scintillation techniques. Using an in-house computer program, the PBMC data analysis includes the calculation of IC50 (50% inhibition of virus replication), IC90 (90% inhibition of virus replication), IC95 (95% inhibition of virus replication) and therapeutic index values (TI = TC/IC; also referred to as Antiviral Index or AI).

OSU-03012 PK/PD studies in brain.—Mice were given an IV bolus (10 mg/kg) of OSU-03012 and 27 brain samples taken (10 mg/kg in a mouse is the equivalent of a single 600 mg drug dose in patients; 800 mg BID was shown to be safe in patients). Tissues were collected and stored at -80°C . They were then weighed, minced into small pieces, and mixed with PBS when ready for analysis. Approximately 50 mg of the frozen mouse brain was crudely homogenized and spiked with 30 μl OSU-03012 solution (acetonitrile/water, 50:50) at appropriate concentrations to give final concentrations of OSU-03012 at 0, 0.06, 0.11, 0.22, 0.56, 1.11, 2.22, 5.56, 11.12, 22.25 nmole/g (or 0, 5, 10, 20, 50, 100, 200, 500, 1000 ng/ml) and a fixed 10 μl (10 $\mu\text{g/ml}$) OSU-Arg (OSU-03013, NSC 728210) as the internal standard. The tissue mixture was then homogenized again in an ice-water bath. Lysis buffer (20 mM Tris pH 8, 20 mM EDTA, 0.5% NP-40) was added to each vial, vortexed and cooled. The mixture was then centrifuged at 14,000 rpm in a bench top microfuge for 2 min, the supernatant transferred to a new vial, and extracted with ethyl acetate (1200 μl , 60 min). The extract layer was separated, transferred to a glass tube, and then dried under a stream of N_2 . The residue is then be reconstituted in 100 μl mobile phase (acetonitrile/water 50:50), centrifuged at 14,000 rpm for 2 min, and a 20 μl aliquot will be injected into the LC-MS/MS instrument.

Data analysis.—Comparison of the effects of various treatments was performed using one-way analysis of variance followed by a two tailed Student's *t*-test. Statistical examination of in vivo animal survival data utilized log rank statistical analyses between the different treatment groups. Differences with a *P*-value of <0.05 were considered to be statistically significant. Experiments shown are the means of multiple individual data points from multiple separate experiments ($\pm\text{SEM}$).

Results

Using multiple strains of influenza A and B viruses and the multi-kinase inhibitory drugs OSU-03012, AR-13, sorafenib, and pazopanib as single agents we found that all of the drugs reduced cell lysis / cell killing in the influenza virus infected cells, 24 h after infection (Fig. 1A, $*P < 0.05$) (Booth et al., 2016a). The two drugs that appeared to consistently suppress influenza virus-mediated cell lysis were OSU-03012 and pazopanib. OSU-03012 combined with the phosphodiesterase 5 inhibitor sildenafil (Viagra) to prevent Chikungunya virus-mediated cell lysis and Coxsackievirus B4—mediated cell lysis (Fig. 1B and C).

Treatment of cells with OSU-03012 \pm sildenafil resulted in a rapid dose- and time-dependent reduction in the detection of the ATP binding and ATPase competent chaperone proteins HSP90, GRP78, and HSP70 in fixed in situ cells as judged using an immuno-

fluorescence/in-cell-western technique (Fig. 2A and B) (see Booth et al., 2016a for more detailed analyses, including immuno-fluorescence images). The expression of the small chaperone HSP27, which lacks an ATP binding site, was also reduced by both OSU-03012 and by sorafenib (Fig. 2C). Using proteomic analyses, as reported in Booth et al. (2016a), OSU-03012 associated with multiple chaperone proteins beyond those previously biochemically recognized, as well as the autophagy regulatory kinase and HSP90 client, ULK-1 (see Booth et al., 2016a for more detailed analyses). OSU-03012 reduced the expression of HSP75, GRP75, HSP27 and the HSP70-associated protein BAG2 (Fig. 3A). In protein-protein co-localization studies OSU-03012 disrupted the association between HSP70 and BAG2; the association between HSP90 and AhA1 as well as the association between the chaperones: HSP70-HSP27; HSP90-HSP70; HSP60-HSP10; and GRP78-GRP94 (Fig. 3B and C). OSU-03012 treatment of cells altered the elution profile of HSP27 from a gel filtration column and the association of GRP78 with PKR-like endoplasmic reticulum kinase following GRP78 immuno-precipitation (Fig. 3D). OSU-03012, sorafenib and pazopanib all exhibited inhibitory effects against the HSP90 ATPase and the HSP70 ATPase activities (Fig. 3E).

Many proteins located in the plasma membrane are also associated with chaperones, for example, ERBB2 and in other studies we observed our drug combinations with sildenafil reducing the levels of multiple receptor tyrosine kinases (Booth et al., 2015a,b, 2016b; Roberts et al., 2015; Tavallai et al., 2015). In the present studies, we next examined the impact of OSU-03012 on the expression of plasma membrane virus receptors. OSU-03012 reduced the expression of the two recognized Ebola virus receptors NPC1 and TIM1 in vitro, an effect that was enhanced by sildenafil (Fig. 4A). Combined overexpression of the chaperones GRP78 and HSP27 enhanced basal expression of the NPC1 and TIM1 receptors and prevented OSU-03012 from reducing NPC1 and TIM1 expression (Fig. 4B, not shown). The replication of DNA and RNA viruses is a complex process requiring many different chaperone proteins, in particular GRP78, and also enzymes involved in the regulation of protein glycosylation; particularly glucosidase I and glucosidase II α/β (De Clercq, 2015; Chang et al., 2013). Treatment of cells with OSU-03012 or with sorafenib rapidly reduced the expression of glucosidase I and glucosidase II α , but did not impact on expression of glucosidase II β (Fig. 4C). Combined over-expression of the chaperones GRP78 and HSP27 prevented the down-regulation of glucosidase I and glucosidase II α , and also the ER transmembrane chaperone Calnexin (Fig. 4D). Of note, overexpression of GRP78 and HSP27 enhanced the basal expression levels of glucosidase I and glucosidase II α .

As OSU-03012 was relieving the inhibitory effect of GRP78 on endoplasmic reticulum stress/PERK signaling we went on and determined that expression of dominant negative eIF2 α S51A blocked OSU-03012—induced expression of the essential autophagy proteins LC3 and Beclin 1 (Fig. 5A) (see Park et al., 2008 and Booth et al., 2016a for more detailed analyses). We have previously published that OSU-03012 stimulates a PERK-dependent form of autophagy (Park et al., 2008). The formation of autophagosomes is also regulated by PI3K pathway signaling, particularly the kinase mTOR. Of note were the side-by-side comparisons of AKT Threonine 308 phosphorylation and mTOR Serine 2448 phosphorylation. As we have previously shown for AKT Threonine 308 phosphorylation, OSU-03012 as a single agent had little to no obvious effect on T308 phosphorylation levels

(Fig. 5B). In contrast, OSU-03012 as a single agent strongly reduced mTOR Serine 2448 phosphorylation. Thus our data argues that OSU-03012 causes a greater degree of mTOR dephosphorylation when compared to its more modest effect on AKT dephosphorylation, implying that the regulation of mTOR activity by the drug is likely to be more biologically important than that of AKT.

The protein kinase ULK-1 is also considered to be an essential gate-keeper kinase for the regulation of autophagosome formation, and whose activity is negatively regulated by Serine 757 phosphorylation catalyzed by the upstream kinase mTOR. OSU-03012 reduced the phosphorylation of mTOR at Serine 2448, indicative of mTOR inactivation (Fig. 5B). (see Booth et al., 2016a for more detailed analyses). Reduced mTOR S2448 phosphorylation correlated with reduced phosphorylation of ULK-1 at Serine 757, as well as appearing to reduce the total expression of ULK-1 protein, which collectively in turn correlated with increased phosphorylation of the autophagosome formation essential regulatory protein ATG13 at Serine 318. Serine 318 phosphorylation of ATG13 facilitates, together with other protein-protein interaction events, autophagosome formation. Transfection of cells to express GRP78 both reduced basal phosphorylation levels and prevented the drug-induced phosphorylation of eIF2 α and ATG13, but did not prevent drug-induced dephosphorylation of mTOR (Fig. 5C). Transfection of cells to express HSP27 prevented OSU-03012 single agent—induced phosphorylation of eIF2 α and ATG13, and prevented the OSU-03012/sorafenib single agent x2014;induced dephosphorylation of mTOR (for data in Fig. 5, please see Booth et al., 2016a for more detailed analyses).

We next performed immuno-fluorescence protein co-localization studies to determine whether phospho-ATG13 S318 or HSP27/GRP78/HSP90 co-localized with the autophagosome vesicle protein LC3 (ATG8) after drug exposure. Treatment of cells for 3 h with OSU-03012 caused phospho-ATG13 S318 or HSP27 to co-localize with LC3 in punctate bodies (Fig. 5D). Treatment of cells for 3 h with OSU-03012 caused GRP78 to co-localize with the autophagosome vesicle marker protein LC3 (Fig. 5D). In contrast, HSP90 and LC3 did not co-associate prior to or after drug exposure. Thus we conclude it is the combined dysregulation of both GRP78 and HSP27 that is required for drug-induced promotion of the autophagy signal. Finally, we determined the impact of knocking down chaperone expression on the ability of OSU-03012 to promote autophagosome formation, using as a read-out the number of LC3-GFP punctae per transfected cell. Combined knock down of (GRP78 and HSP27) or of (HSP90 and HSP70) significantly increased the basal levels of autophagosomes in cells and significantly reduced the ability of OSU-03012 to further stimulate autophagosome production when compared to scramble control transfected cells (Fig. 5E, $P < 0.05$).

As OSU-03012 was down-regulating the functionality of multiple chaperone proteins, we next determined whether molecular genetic manipulation of chaperone expression in combination could further reduce the ability of viruses to replicate. Cells in vitro were transfected with various siRNA molecules and 24 h afterwards infected with virus followed by assessment of cell viability 24 and 48 h after virus infection. Individual knock down of HSP27, GRP78, or GRP75 prevented Influenza A and Influenza B viruses from causing cell

death, whereas knock down of BAG2 or HSP75 were only partially protective (Fig. 6A and B).

In prior studies we noted that GRP78 is inhibited by OSU-03012 and that the resulting endoplasmic reticulum stress signal causes the expression of LC3 and Beclin 1 to be enhanced in a PERK-dependent fashion (Park et al., 2008; Booth et al., 2012, 2016a). We hypothesized that the ability of OSU-03012 to induce autophagosome formation was also causal in the abilities of this drug treatment to act as an anti-viral agent. As previously shown by us for multiple other epithelial and fibroblast cell types, knock down of Beclin 1 suppressed the ability of OSU-03012 to induce the formation of autophagosomes in MRC5 and other cell types (see Fig. 5E). Knock down of Beclin 1 also reduced the ability of OSU-03012 to prevent Influenza A and Influenza B viruses from killing MRC5 cells (Fig. 7A, $P < 0.05$). A non-significant trend was also observed where knock down of Beclin 1 itself appeared to slightly reduce virus lethality ($P < 0.29$). Treatment of influenza virus infected cells with OSU-03012 caused the co-localization of virus proteins (using the anti-Influenza A/B virus rabbit polyclonal antibody M149 from Clontech) with the autophagosome marker LC3, (Fig. 7B and C). Cells infected with either Influenza A or Influenza B viruses exhibited several large vesicle structures that stained with the M149 antibody and treatment of cells with OSU-03012 significantly increased the mean number of virus protein containing vesicles from 6.3 per cell to 16.8 per cell (Fig. 7D, $P < 0.05$). In co-localization studies, in cells infected with Influenza A, OSU-03012 caused the co-localization of LC3 and GRP78 and of LC3 and HSP27, that is, chaperones were associated with autophagosomes (Fig. 7E). However, Influenza B infected cells treated with OSU-03012 did not exhibit the LC3 and HSP27 co-localization effect.

We next determined the effects of (OSU-03012 + sildenafil) as well as molecular modulation of GRP78 and HSP27 on the reproductive cycle of Coxsackievirus B4. In a dose-dependent fashion Coxsackievirus B4 killed cells; an effect that was prevented by post-infection treatment of the cells with (OSU-03012 + sildenafil) (Fig. S1A). Over-expression of GRP78 enhanced virus lethality and partially abrogated the protective effect of (OSU-03012 + sildenafil) treatment. Knock down of GRP78 suppressed virus-mediated cell lysis (Fig. S1B). Over-expression of HSP27 also enhanced Coxsackievirus B4 lethality, and knock down of HSP27 also reduced virus-induced cell killing at this time point (Fig. S1C).

Again using Coxsackievirus B4, 24 h after infection, knock down of HSP27, BAG2, GRP75, HSP75, or GRP78 modestly suppressed virus-mediated cell killing (Fig. 8A). Combined knock down of GRP78 with each of the other chaperone proteins almost abolished cell killing at the 24 h time point. Forty eight hours after infection knock down of GRP78 caused a large reduction in cell killing as did to a lesser extent that of HSP27 and HSP75. Combined knock down of GRP78 with either HSP27 or HSP75 resulted in a further decline in virus-mediated cell death. In parallel studies we infected cells 24 h after siRNA transfection with Mumps virus. In cells infected with Mumps virus, 24 h after infection, knock down of HSP27, BAG2, GRP75, HSP75, or GRP78 suppressed virus-mediated cell killing (Fig. 8B). Combined knock down of GRP78 with other chaperone proteins did not appear to significantly reduce virus cell killing at this time point. Forty-eight hours after infection, only knock down of GRP78 or HSP27 alone significantly reduced virus-mediated cell death.

Combined knock down of GRP78 and HSP27 virtually abolished Mumps virus lethality. Combined knock down of GRP78 and HSP27 also prevented the replication of Measles virus and of Rubella virus (Fig. 5C). The data in Figure 8D shows control studies for knock down of the different chaperone proteins.

Human macrophages were transfected with a plasmid, purchased from Addgene, to simultaneously express four Human Immuno-deficiency virus (HIV) proteins (Gag/Pol, Tat, Rev). Twenty-four h after transfection cells were treated with OSU-03012 and the co-localization of virus proteins with chaperones and LC3 determined. As was observed for the Influenza virus proteins, we observed increased HIV protein co-localization with LC3 after drug exposure and decreased HIV protein co-localization with HSP70 and GRP78 (Fig. 9A-C). Standard of care treatment of HIV patients use a combination of three protease inhibitors to impede virus replication, maturation and release. Unfortunately, as with many drugs designed to inhibit viral protein function which target mutable viral proteins, the evolutionary selective pressure of the drug results in the outgrowth of mutant resistant strains; and sadly the HIV genome is no exception to this evolutionary pressure. AR-12 exhibited a dose-dependent reduction in virus replication for all virus isolates tested, with an average IC50 value of 812 nM (IC50 range = 489 nM to 1,016 nM) (Tables 1 and 2). However, there was no apparent resistance to AR-12 for any of the HIV drug resistant isolates evaluated in this study. These findings strongly suggest that AR-12 inhibits HIV replication/infection through a mechanism that is different from the NRTI, NNRTI, PI, INI and entry inhibitors to which these isolates are resistant.

Epstein-Barr virus (EBV) is the virus responsible for mononucleosis (glandular fever) but also can play a role in promoting cancer, particularly in lymphoid tissues as well as in the stomach and naso-pharyngeal passages. We determined the impact of OSU-03012 on the co-localization of EBNA1 (in the panel, EBV1) and LMP latent protein (in the panel, EBV2) with HSP90, HSP70, GRP78, and LC3. We also examined the co-localization of the recognized EBV receptor proteins CD19 (in the panel, EBV3) and CD21 (in the panel, EBV4) with HSP90, HSP70, GRP78, and LC3. In both Raji and Dakiki EBV infected lymphoblastoma B-cells, OSU-03012 caused the co-localization of the EBNA1 (EBV1) and LMP-1 (EBV2) viral proteins with the autophagosome marker LC3 (Figs. S2-S5). The OSU-03012 drug treatment also caused the localization of the receptors CD19 and CD21 with LC3 in the autophagosomes. EBNA1, LMP-1, CD19, and CD21 all were chaperoned by HSP90 under control conditions whereas after OSU-03012 treatment their co-localization with the chaperone was abolished. The association of EBNA-1, LMP-1, CD19, and CD21 with HSP70 appeared to be less intense than the association we observed for HSP90; however, data from both cell lines strongly argued that OSU-03012 treatment reduced the co-localization of HSP70 with our EBV proteins. Our findings examining the association of EBNA1, LMP-1, CD19 and CD21 with GRP78 were very similar to those observed using HSP90; all four EBV related proteins co-localized with GRP78 under control conditions, an interaction which was abolished by OSU-03012 treatment.

Treatment of Ebola virus infected cells with OSU-03012 suppressed the replication of Ebola virus in vitro, in agreement with data recently reported by others (Fig. 10A) (Reid et al., 2014; Mohr et al., 2015). Individual knock down of GRP78 or of HSP75 also significantly

reduced Ebola virus replication in vitro in HeLa cells (Fig. 10B). This is in general agreement with published data showing that molecular knock down of GRP78 in vivo prolongs the survival of mice infected with Ebola virus (Reid et al., 2014). In vivo, treatment of athymic mice with OSU-03012 significantly reduced the expression of Ebola virus TIM1 and NPC1 receptors in both the brain and the liver (Fig. 10C). Furthermore, when mice were given an IV bolus (10 mg/kg, the equivalent of a single 600 mg drug dose in patients) of OSU-03012 and brain samples taken, we demonstrated that OSU-03012 crossed the blood brain barrier within 5 min of IV dosing, with a peak brain concentration of 2 μ M within 240 min (Fig. 10D). It should be noted in the phase I trial using OSU-03012 the safe tolerated dose was determined to be 800 mg BID (NCT00978523). In the mouse brain, treatment of the animal with (OSU-03012 + sildenafil) reduced the expression of GRP78 and the blood-brain barrier drug efflux pumps ABCB1 and ABCG2 (gross 10 \times magnification images). OSU-03012 was still detectable in mouse brain tissue 48 h after dosing (gross 10 \times magnification images). Treatment of animals with (OSU-03012 + sildenafil) did not cause any apparent normal tissue toxicity as judged by H&E staining (data not shown).

Additional studies next examined the replication of different strains of Junin virus (JUNV), agent of Argentine hemorrhagic fever, was potently inhibited by treatment with OSU-03012 (AR-12) in both human A549 and monkey Vero cells. OSU-03012 (AR-12) was more effective against all JUNV strains than ribavirin, the reference drug for arenaviral hemorrhagic fever, with significantly higher selectivity indices (Fig. 11A). By immunofluorescence staining of viral nucleoprotein NP, JUNV infected cells expressing NP were also drastically reduced (Fig. 11B). In chaperone knockdown studies, cells were transfected with various siRNAs and 24 h later infected with JUNV, virus infectivity was then determined after 24 and 72 h of infection. Individual knockdown of HSP90 significantly reduced the replication of JUNV at 24 h post-infection, whereas the silencing of GRP78 and HSP70 also produced virus inhibition but at a minor level (Fig. 11C). Based on our control knock down data using these siRNA molecules herein and other studies, the mole/mole effectiveness of each siRNA against its individual target was nearly identical between the targets. Seventy-two hours after infection a similar response was detected. When combination of the three more effective siRNAs was tested, only the simultaneous knockdown of HSP90 and HSP70 resulted in higher reduction in virus infectivity (Fig. 11C). The JUNV infectivity results regarding chaperone knockdown were confirmed by immunofluorescence staining of viral NP in the siRNA transfected infected cells (Fig. 11D).

Finally, based on our in vitro data with the Ebola and Junin hemorrhagic viruses, we determined whether OSU-03012 could prolong the survival of animals infected with another hemorrhagic fever virus, the rabbit hemorrhagic disease virus (RHDV), which is an accepted model of fulminant viral hepatitis in humans (San-Miguel et al., 2006; Tunon et al., 2011). For these studies we used transient low dosing levels of OSU-03012, compared to our prior tumor survival studies in glioblastoma (Booth et al., 2012). Rabbits infected with virus and vehicle control-treated began to die 36 h after infection and 60 h after infection approximately 70% of the animals had died (Fig. 12). Animals treated with OSU-03012 began to die 48 h post-infection and 60–72 h post-infection approximately 30% of the animals had died, a doubling of the survival effect that was found to be statistically significant ($P < 0.05$). In parallel studies examining the plasma of rabbits after RHDV

infection we discovered OSU-03012 significantly reduced the virus-induced increases in plasma ALT, LDH, and GGT levels (Fig. 13). In agreement with longer survival and reduced liver damage, animals treated with OSU-03012 exhibited less expression of virus protein VP60 mRNA at the time of animal nadir, which correlated with reduced obvious liver damage assessed by H&E staining of liver sections (Fig. 14).

Discussion

At present OSU-03012 (AR-12) has orphan drug designation in Europe for the treatment of *cryptococcosis* and *tularaemia*, and the licensees of OSU-03012, Arno Therapeutics, has entered into a cooperative research and development agreement with the US Army Medical Research Institute of Infectious Diseases for AR-12. Ourselves and others have shown that OSU-03012 (AR-12) has anti-tumor activity in vitro and in vivo in many model systems as well as having anti-viral and anti-bacterial properties against organisms as diverse as Mumps, Measles, Influenza, Ebola, Marburg, and pan-antibiotic resistant strains of *Neisseria gonorrhoea* and *Klebsiella pneumoniae*.

Chaperone proteins play essential roles in the biology of tumor cells that express high protein levels, but also are essential for pathogenic viruses to safely and effectively reproduce in eukaryotic cells. In particular, the chaperone GRP78 has been linked since the late 1980s in tens of studies as a protein essential for viral replication (e.g., Lee, 2007; Ni and Lee, 2007; Luo and Lee, 2013; Tsai et al., 2015). Other studies have shown additional chaperones including HSP90 and HSP27 as proteins which facilitate the viral life cycle. Chaperone expression is essential in virus life cycles for several reasons: (a) GRP78 and other chaperones are essential for correct 2^o/3^o protein folding of nascent viral peptides in the endoplasmic reticulum, including viral core protein expression; (b) elevated GRP78 levels as well as the levels of other chaperone proteins upon viral infection together with virus-mediated dephosphorylation of eIF2 α collectively prevent a profound intense endoplasmic reticulum stress response being generated after viral infection which thus prevents cell death prior to the replication of genetic material and the formation of progeny viruses; (c) the chaperones GRP94, HSP90, HSP70, HSP60, and HSP27 have all each been shown in a variety of virus types to play secondary roles in the replication of viral genetic material as well as the formation of new viral capsid complexes (Gober et al., 2005; Mathew et al., 2009; Liu et al., 2014; Vashist et al., 2015; Zhang et al., 2015). Thus as AR-12 simultaneously dysregulates the functionality of multiple chaperone proteins, this compound will profoundly act to block the production and reduce the stability of many essential viral proteins required for virus reproduction.

But, in addition to its anti-chaperone effects that impact the production and stability of viral proteins, AR-12 also, through chaperone inhibition, provokes a host cell endoplasmic reticulum stress response which elevates Beclin 1 and LC3 levels in parallel with causing the inactivation of mTOR and phosphorylation of ATG13 S318; and that together facilitate the production of autophagosomes. We demonstrated that chaperone proteins are associated with viral proteins under control conditions and that chaperone proteins do not co-localize with the few autophagosomes present in control cells. After AR-12 exposure, however, virus proteins and chaperone proteins have become localized in the greater AR-12—stimulated

number of autophagosomes, and that under these conditions the co-localization of virus protein with chaperone protein has declined. Thus AR-12 acts through two over-arching mechanisms to prevent the production of progeny virus. This first mechanism is to reduce the infection, production, and stability of virus proteins including reduced intracellular processing, and the second through stimulating the production of autophagosomes who in turn act to sequester the denatured viral proteins where these proteins will eventually be degraded in the autolysosomes.

Contemporaneously with our own AR-12 anti-tumor and anti-viral studies, two other groups of researchers demonstrated that the expression of GRP78 was essential for Ebola virus reproduction in vitro going on to show that molecular knock down of GRP78 in vivo protected mice from Ebola virus lethality, and that OSU-03012 prevented the replication of many hemorrhagic fever viruses in vitro, including Ebola, Lassa and Marburg (Reid et al., 2014; Mohr et al., 2015). The present studies demonstrate that molecular knock down of several AR-12 interacting chaperone proteins, alone or in combination, could also prevent the replication of life-threatening viruses such as Influenza, Measles, and Ebola. Several years ago a phase I trial in heavily pre-treated cancer patients treated with increasing doses of OSU-03012 was reported (NCT00978523; J. Clin. Oncol. 31,2013 suppl; abstr 2608). The drug plasma C_{max} was approximately 8 μ M for a safe 800 mg BID dosing, and some patients with stable disease remained on the trial for up to 33 weeks. That is, our pre-clinical studies use the drug at 20% or less of the achievable plasma level. The major pharmacological issue to come out of this trial over further development for AR-12 was a need for its reformulation, to standardize drug uptake/PK/PD in patients. As AR-12 is orally ingested, and based on our data of the last 12 months, it seems obvious that AR-12, particularly if combined with sildenafil, should be deployed for the treatment of life threatening infections such as Influenza, Junin, Measles, and Ebola.

In our very recent mechanistic/biochemical Booth et al. (2016a) manuscript, when using antibodies raised against epitopes in different portions of HSP90, HSP70, HSP27, and GRP78 we observed discordant data, using immunofluorescence detection. Antibodies raised against the ATP-binding NH_2 -terminal domains of HSP90, HSP70, and GRP78 demonstrated that OSU-03012 treatment reduced chaperone immuno-fluorescence detection whereas those antibodies raised against central and $COOH$ -terminal epitopes remained constant or exhibited more modest declines in detection (Booth et al., 2016a). Data using bacterial and eukaryotic expressed chaperones also strongly argued that OSU-03012 was interacting with chaperone proteins through the ATP binding site within their ATPase domain and that this modified chaperone-client interactions. Proteomic data in Booth et al. (2016a) demonstrated that OSU-03012 interacted with multiple other ATP, GTP and purine binding proteins, thus a portion of the mechanism by which OSU-03012 suppresses influenza virus replication could have similarities to that of Ribavirin. In Figure 1 we demonstrated that the analogue of OSU-03012, AR-13, also had anti-viral properties. In Booth et al. (2016a), AR-13 was at the very least equipotent at inhibiting chaperone ATPase activities in vitro as was OSU-03012. And we thus concluded that the phenanthrene system in both AR-12 and in AR-13 is essential for their enhanced biological activities toward chaperones compared to their parent compound celecoxib.

In conclusion, AR-12 (OSU-03012) interacts with multiple chaperone proteins of the HSP90 family and the HSP70 family resulting in a broad spectrum of chaperone inactivation. This overall loss of chaperone functionality results in cells being more readily capable of undergoing autophagic processes and in cells that have a reduced competency for virus replication. AR-12 and pazopanib both have modest normal tissue toxicities in comparison to anti-viral drugs such as AZT or the HIV protease inhibitors and as such, they could represent a novel wide-ranging basis for treating RNA and DNA virus infections as well as viral-induced human malignancies, for example, by EBV.

Supplementary Material

Refer to Web version on PubMed Central for supplementary material.

Acknowledgments

Thanks to Dr. H.F. Young (Neurosurgery, VCU) and the Betts family fund for support in the purchase of the Hermes Wiscan instrument. PD wishes to thank Mr. Daniel Leon (VCU personnel, Dent laboratory) for assistance during these studies. Support for the present study was funded by philanthropic monies supplied by Massey Cancer Center (to PD). Services in support of the research project were provided by the VCU Massey Cancer Center Tissue and Data Acquisition and Analysis Core, supported, in part, with funding from NIH-NCI Cancer Center Support Grant P30 CA016059. The HIV viral replication studies were conducted in part (or in total) by Southern Research Institute using federal funds from the Division of AIDS, National Institute of Allergy and Infectious Diseases, National Institutes of Health under contract HHSN27220I4000I0I entitled "In Vitro Testing Resources for HIV Therapeutics and Topical Microbicides."

Contract grant sponsor: Massey Cancer Center.

Contract grant sponsor: NIH-NCI Cancer Center;

Contract grant number: P30 CA016059.

Contract grant sponsor: Division of AIDS, National Institute of Allergy and Infectious Diseases, National Institutes of Health; Contract grant number: HHSN2722014000101.

Abbreviations:

CAR	coxsackie and adenovirus receptor
CD	cluster of differentiation
OSU	OSU-03012 also called AR-12
SIL	sildenafil also called Viagra
TAD	tadalafil also called Cialis
PTEN	Phosphatase and tensin homolog
R	receptor
dn	dominant negative
CMV	empty vector control plasmid
COX	cyclooxygenase

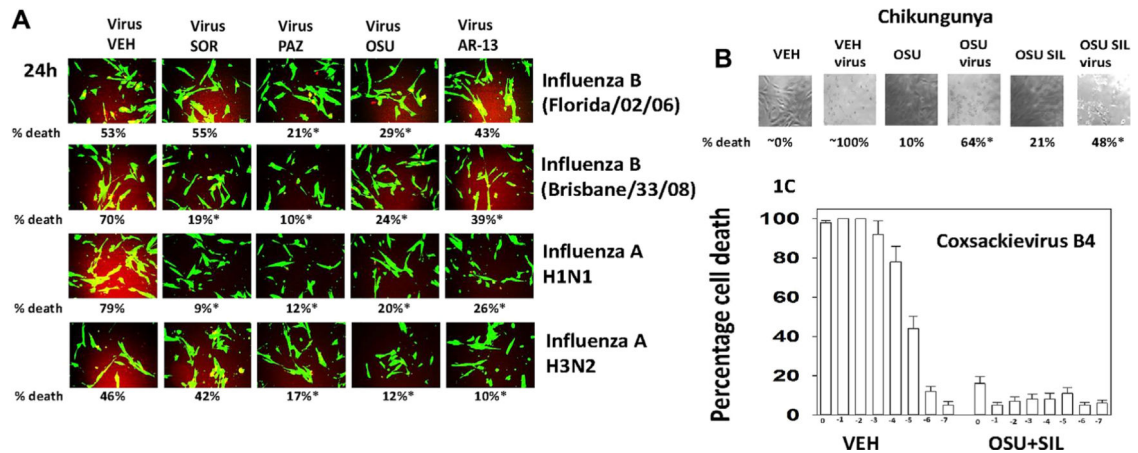
P	phospho
ca	constitutively active
WT	wild type
PERK	PKR like endoplasmic reticulum kinase
HSP	heat shock protein
GRP	glucose regulated protein

Literature Cited

- Anderson K, Stott EJ, Wertz GW. 1992 Intracellular processing of the human respiratory syncytial virus fusion glycoprotein: Amino acid substitutions affecting folding, transport and cleavage. *J Gen Virol* 73:1177–1188. [PubMed: 1375280]
- Bolt G 2001 The measles virus (MV) glycoproteins interact with cellular chaperones in the endoplasmic reticulum and MV infection upregulates chaperone expression. *Arch Virol* 146:2055–2068. [PubMed: 11765911]
- Booth L, Cazanave SC, Hamed HA, Yacoub A, Ogretmen B, Chen CS, Grant S, Dent P. 2012 OSU-03012 suppresses GRP78/BiP expression that causes PERK-dependent increases in tumor cell killing. *Cancer Biol Ther* 13:224–236. [PubMed: 22354011]
- Booth L, Roberts JL, Cruickshanks N, Grant S, Poklepovic A, Dent P. 2014 Regulation of OSU-03012 toxicity by ER stress proteins and ER stress-inducing drugs. *Mol Cancer Ther* 13:2384–2398. [PubMed: 25103559]
- Booth L, Roberts JL, Tavallai M, Nourbakhsh A, Chuckalovcak J, Carter J, Poklepovic A, Dent P. 2015a. OSU-03012 and viagra treatment inhibits the activity of multiple chaperone proteins and disrupts the blood-brain barrier: Implications for anti-cancer therapies. *J Cell Physiol* 230:1982–1998.
- Booth L, Roberts JL, Cash DR, Tavallai S, Jean S, Fidanza A, Cruz-Luna T, Siembiba P, Cycon KA, Cornelissen CN, Dent P. 2015b GRP78/BiP/HSPA5/Dna K is a universal therapeutic target for human disease. *J Cell Physiol* 230:1661–1676. [PubMed: 25546329]
- Booth L, Shuch B, Albers T, Roberts JL, Tavallai M, Proniuk S, Zukiwski A, Wang D, Chen CS, Bottaro D, Ecroyd H, Lebedyeva IO, Dent P. 2016a Multi-kinase inhibitors can associate with heat shock proteins through their NH2-termini by which they suppress chaperone function. *Oncotarget* 7:12975–12996. [PubMed: 26887051]
- Booth L, Roberts JL, Tavallai M, Webb T, Leon D, Chen J, McGuire WP, Poklepovic A, Dent P. 2016b The afatinib resistance of in vivo generated H1975 lung cancer cell clones is mediated by SRC/ERBB3/c-KIT/c-MET compensatory survival signaling. *Oncotarget* 7:19620–19630 [PubMed: 26934000]
- Booth L, Roberts JL, Tavallai M, Chuckalovcak J, Stringer DK, Koromilas AE, Boone DL, McGuire WP, Poklepovic A, Dent P. 2016c [Pemetrexed+Sorafenib] lethality is increased by inhibition of ERBB1/2/3-PI3K-NFκB compensatory survival signaling. *Oncotarget* 7:23608–23632 [PubMed: 27015562]
- Buckheit RW, Jr., Swanstrom R 1991 Characterization of an HIV-I isolate displaying an apparent absence of virion-associated reverse transcriptase activity. *AIDS Res Hum Retroviruses* 7:295–302. [PubMed: 1712216]
- Caron RW, Yacoub A, Li M, Zhu X, Mitchell C, Hong Y, Hawkins W, Sasazuki T, Shirasawa S, Kozikowski AP, Dennis PA, Hagan MP, Grant S, Dent P. 2005 Activated forms of H-RAS and K-RAS differentially regulate membrane association of PI3K, PDK-I, and AKT and the effect of therapeutic kinase inhibitors on cell survival. *Mol Cancer Ther* 4:257–270. [PubMed: 15713897]
- Chang J, Block TM, Guo JT. 2013. Antiviral therapies targeting host ER alpha-glucosidases: Current status and future directions. *Antiviral Res* 99:251–260. [PubMed: 23816430]

- Dabo S, Meurs EF. 2012 DsRNA-dependent protein kinase PKR and its role in stress, signaling and HCV infection. *Viruses* 4:2598–2635. [PubMed: 23202496]
- De Clercq E 2015 Ebola virus (EBOV) infection: Therapeutic strategies. *Biochem Pharmacol* 93:1–10. [PubMed: 25481298]
- Dimcheff DE, Faasse MA, McAtee FJ, Portis JL. 2004 Endoplasmic reticulum (ER) stress induced by a neurovirulent mouse retrovirus is associated with prolonged BiP binding and retention of a viral protein in the ER. *J Biol Chem* 279:33782–33790. [PubMed: 15178688]
- Earl PL, Moss B, Doms RW. 1991 Folding, interaction with GRP78-BiP, assembly, and transport of the human immunodeficiency virus type 1 envelope protein. *J Virol* 65:2047–2055. [PubMed: 1900540]
- Gao M, Yeh PY, Lu YS, Hsu CH, Chen KF, Lee WC, Feng WC, Chen CS, Kuo ML, Cheng AL. 2008 OSU-03012, a novel celecoxib derivative, induces reactive oxygen species-related autophagy in hepatocellular carcinoma. *Cancer Res* 68:9348–9357. [PubMed: 19010909]
- Gober MD, Wales SQ, Aurelian L. 2005 Herpes simplex virus type 2 encodes a heat shock protein homologue with apoptosis regulatory functions. *Front Biosci* 10:2788–2803. [PubMed: 15970534]
- Goodwin EC, Lipovsky A, Inoue T, Magaldi TG, Edwards AP, Van Goor KE, Paton AW, Paton JC, Atwood WJ, Tsai B, DiMaio D. 2011 BiP and multiple DNAJ molecular chaperones in the endoplasmic reticulum are required for efficient simian virus 40 infection. *MBio* 2: e00101–e00111. [PubMed: 21673190]
- Hogue BG, Nayak DP. 1992. Synthesis and processing of the influenza virus neuraminidase, a type II transmembrane glycoprotein. *Virology* 188:510–517. [PubMed: 1585634]
- Lee AS. 2007 GRP78 induction in cancer: Therapeutic and prognostic implications. *Cancer Res* 67:3496–3499. [PubMed: 17440054]
- Liu J, Zhang L, Zhu X, Bai J, Wang L, Wang X, Jiang P. 2014 Heat shock protein 27 is involved in PCV2 infection in PK-15 cells. *Virus Res* 189:235–242. [PubMed: 24907481]
- Luo B, Lee AS. 2013 The critical roles of endoplasmic reticulum chaperones and unfolded protein response in tumorigenesis and anticancer therapies. *Oncogene* 32:805–818. [PubMed: 22508478]
- Mathew SS, Della Selva MP, Burch AD. 2009 Modification and reorganization of the cytoprotective cellular chaperone Hsp27 during herpes simplex virus type 1 infection. *J Virol* 83:9304–9312. [PubMed: 19587060]
- Mirazimi A, Svensson L. 2000 ATP is required for correct folding and disulfide bond formation of rotavirus VP7. *J Virol* 74:8048–8052. [PubMed: 10933714]
- Mohr EL, McMullan LK, Lo MK, Spengler JR, Bergeron E, Albarrno CG, Shrivastava-Ranjan P, Chiang CF, Nichol ST, Spiropoulou CF, Flint M. 2015 Inhibitors of cellular kinases with broad-spectrum antiviral activity for hemorrhagic fever viruses. *Antiviral Res* 120:40–47. [PubMed: 25986249]
- Ni M, Lee AS. 2007 ER chaperones in mammalian development and human diseases. *FEBS Lett* 581:3641–3651. [PubMed: 17481612]
- Park MA, Yacoub A, Rahmani M, Zhang G, Hart L, Hagan MP, Calderwood SK, Sherman MY, Koumenis C, Spiegel S, Chen CS, Graf M, Curiel DT, Fisher PB, Grant S, Dent P. 2008 OSU-03012 stimulates PKR-like endoplasmic reticulum-dependent increases in 70-kDa heat shock protein expression, attenuating its lethal actions in transformed cells. *Mol Pharmacol* 73:1168–1184. [PubMed: 18182481]
- Rathore APS, Ng ML, Vasudevan SG. 2013 Differential unfolded protein response during Chikungunya and Sindbis virus infection: CHIKV nsP4 suppresses eIF2 α phosphorylation. *Virol J* 10:36. [PubMed: 23356742]
- Reid SP, Shurtleff AC, Costantino JA, Tritsch SR, Retterer C, Spurgers KB, Bavari S. 2014 HSPA5 is an essential host factor for Ebola virus infection. *Antiviral Res* 109:171–174. [PubMed: 25017472]
- Roberts JL, Tavallai M, Nourbakhsh A, Fidanza A, Cruz-Luna T, Smith E, Siembida P, Plamondon P, Cycon KA, Doern CD, Booth L, Dent P. 2015. GRP78/Dna K is a target for Nexavar/Stivarga/Votrient in the treatment of human malignancies, viral infections and bacterial diseases. *J Cell Physiol* 230:2552–2578.
- Roux L 1990 Selective and transient association of Sendai virus HN glycoprotein with BiP. *Virology* 175:161–166. [PubMed: 2155507]

- San-Miguel B, Alvarez M, Culebras JM, Gonzalez-Gallego J, Tunon MJ. 2006 N-acetyl- cysteine protects liver from apoptotic death in an animal model of fulminant hepatic failure. *Apoptosis* 11: 1945–1957.
- Tavallai M, Hamed HA, Roberts JL, Cruickshanks N, Chuckalovcak J, Poklepovic A, Booth L, Dent P. 2015 Nexavar/Stivarga and viagra interact to kill tumor cells. *J Cell Physiol* 230:2281–2298. [PubMed: 25704960]
- Tsai YL, Zhang Y, Tseng CC, Stanciauskas R, Pinaud F, Lee AS. 2015 Characterization and mechanism of stress-induced translocation of 78-kilodalton glucose-regulated protein (GRP78) to the cell surface. *J Biol Chem* 290:8049–8064. [PubMed: 25673690]
- Tunon MJ, Sanchez-Campos S, Garcia-Ferreras J, Álvarez M, Jorquera F, Gonzalez-Gallego J. 2003 Rabbit hemorrhagic viral disease: Characterization of a new animal model of fulminant liver failure. *J Lab Clin Med* 141:272–278. [PubMed: 12677173]
- Tunon MJ, San-Miguel B, Crespo I, Jorquera F, Santamaria E, Alvarez M, Prieto J, Gonzalez- Gallego J 2011 Melatonin attenuates apoptotic liver damage in fulminant hepatic failure induced by the rabbit hemorrhagic disease virus. *J Pineal Res* 50:38–45. [PubMed: 20964705]
- Vashist S, Urena L, Gonzalez-Hernandez MB, Choi J, de Rougemont A, Rocha-Pereira J, Neyts J, Hwang S, Wobus CE, Goodfellow I. 2015 Molecular chaperone Hsp90 is a therapeutic target for noroviruses. *J Virol* 89:6352–6363. [PubMed: 25855731]
- Xu A, Bellamy AR, Taylor JA. 1998 BiP (GRP78) and endoplasmic (GRP94) are induced following rotavirus infection and bind transiently to an endoplasmic reticulum-localized virion component. *J Virol* 72:9865–9872. [PubMed: 9811722]
- Yacoub A, Park MA, Hanna D, Hong Y, Mitchell C, Pandya AP, Harada H, Powis G, Chen CS, Koumenis C, Grant S, Dent P. 2006 OSU-03012 promotes caspase-independent but PERK-, cathepsin B-, BID-, and AIF-dependent killing of transformed cells. *Mol Pharmacol* 70:589–603. [PubMed: 16622074]
- Zhang C, Kang K, Ning P, Peng Y, Lin Z, Cui H, Cao Z, Wang J, Zhang Y. 2015 Heat shock protein 70 is associated with CSFV NS5A protein and enhances viral RNA replication. *Virology* 482:9–18. [PubMed: 25827528]
- Zhu J, Huang JW, Tseng PH, Yang YT, Fowble J, Shiau CW, Shaw YJ, Kulp SK, Chen CS. 2004 From the cyclooxygenase-2 inhibitor celecoxib to a novel class of 3-phosphoinositide- dependent protein kinase-1 inhibitors. *Cancer Res* 64:4309–4318. [PubMed: 15205346]

**Fig. 1.**

OSU-03012 (AR-12); AR-13; sorafenib tosylate; and pazopanib all are capable of suppressing Influenza A and Influenza B virus replication. A: MRC5 non-transformed human lung fibroblasts were infected with influenza viruses (100 multiplicity of infection). Two hours after infection the cells were treated with vehicle control; sorafenib tosylate (2 μM); pazopanib (2 μM); OSU-03012 (2 μM); and AR-13 (2 μM). Twenty-four hours after infection the cells are treated with live/dead agent where green cells are viable and cells staining yellow or red are considered dead. Cells are examined at 10 \times magnification in a Hermes wide-field microscope ($n = 3 \pm \text{SEM}$) * $P < 0.05$ less than vehicle control level of virus-mediated cell killing. B: VERO cells were infected with Chikungunya virus (100 multiplicity of infection). Two hours after infection the cells were treated with vehicle control; sorafenib tosylate (2 μM); OSU-03012 (2 μM); and sildenafil (2 μM) either alone or in combination. Twenty-four hours after infection the cells were examined under visible light at 10 \times magnification in a Hermes wide-field microscope ($n = 3 \pm \text{SEM}$) * $P < 0.05$ less than vehicle control level of virus-mediated cell killing. C: HEK293 cells (7,000 per well of a 96 well plate) were infected at 1,000 m.o.i. (10^0 value) and with 10-fold dilutions of the virus (10^{-1} — 10^{-7}). Two hours after infection the cells were treated with vehicle control or with (OSU-03012 [2 μM] and sildenafil [2 μM]). Twenty-four hours after infection the cells are treated with live/dead agent where green cells are viable and cells staining yellow or red are considered dead. Cells are examined at 10 \times magnification in a Hermes wide-field microscope (a representative study of 3, all values performed in triplicate $\pm \text{SEM}$).

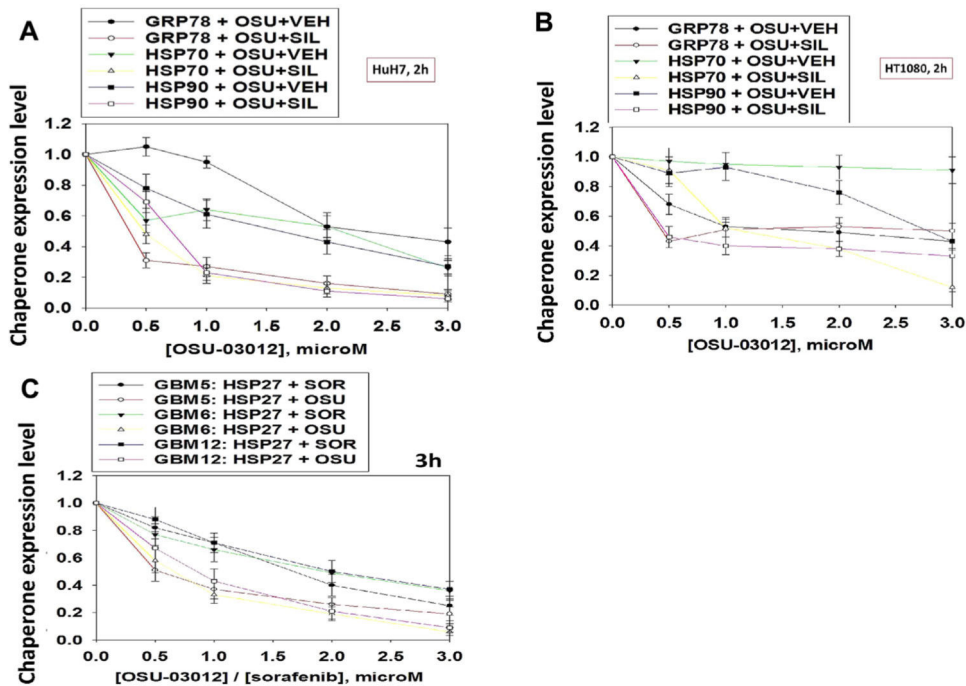
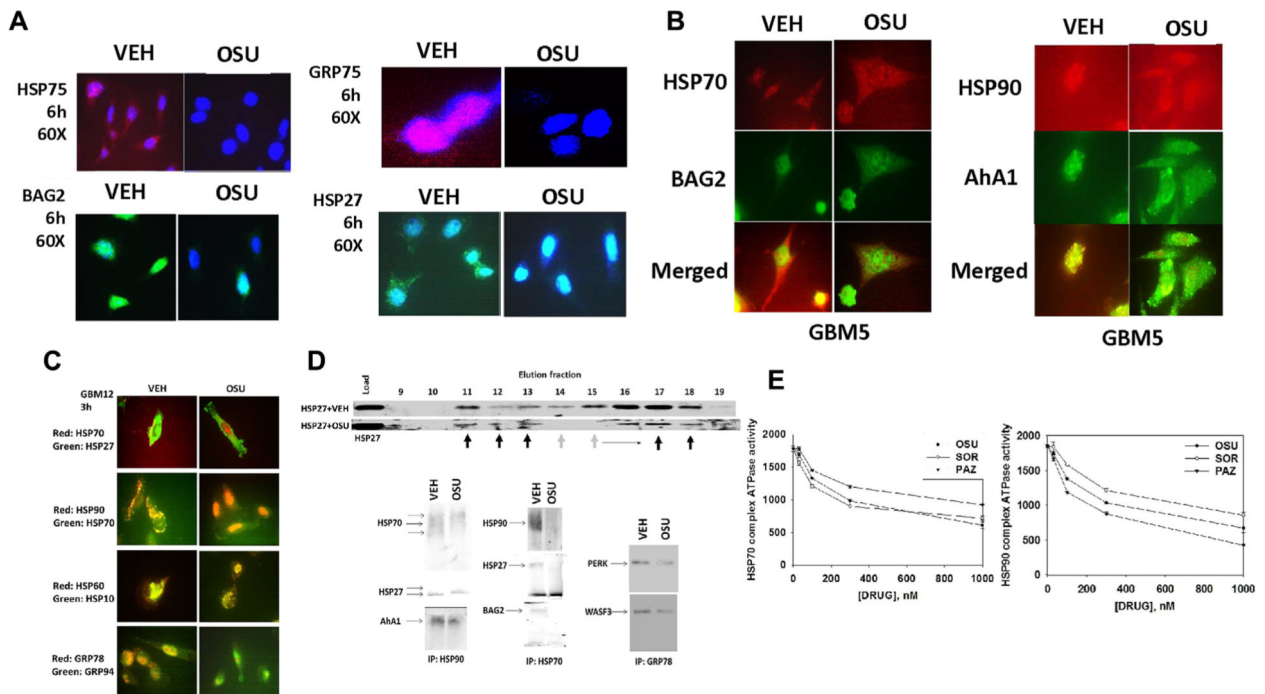


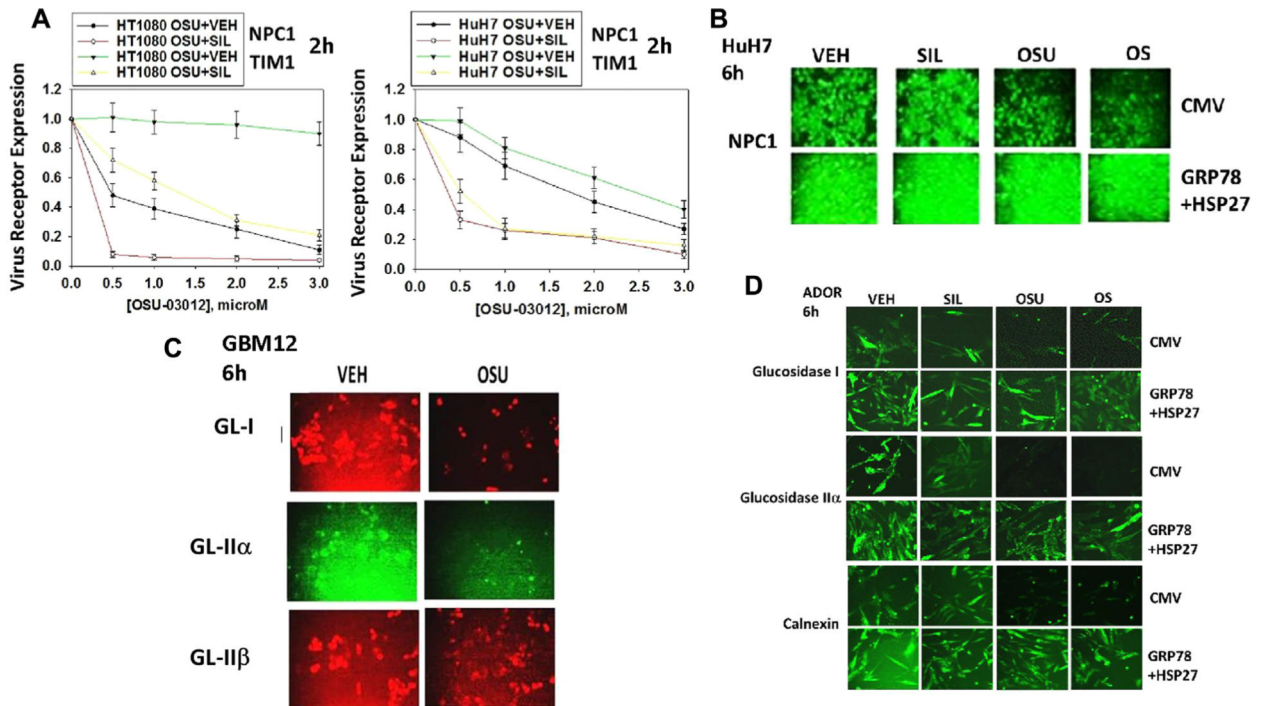
Fig. 2.

OSU-03012 reduces the expression of multiple chaperone proteins, an effect that is enhanced by sildenafil (Please see Booth et al, 2016a). A and B: HuH7 cells and HT1080 were treated with vehicle, OSU-03012 (0–3.0 μM) and/or sildenafil (2 μM) for 2 h after which cells were fixed in place and permeabilized using 0.5% Triton X100. Immunofluorescence was performed to detect the expression levels of GRP78, HSP70, and HSP90. The relative fluorescence intensity value from 40 different cells from each condition was determined using Hermes system software ($n = 3 \pm \text{SEM}$). C: GBM5, GBM6, and GBM12 cells were treated with vehicle, OSU-03012 (0–3.0 μM) or sorafenib (0–3.0 μM) for 3 h after which cells were fixed in place and permeabilized using 0.5% Triton X100. Immunofluorescence was performed to detect the expression level of HSP27. The relative fluorescence intensity value from 40 different cells from each condition was determined using Hermes system software ($n = 3 \pm \text{SEM}$).

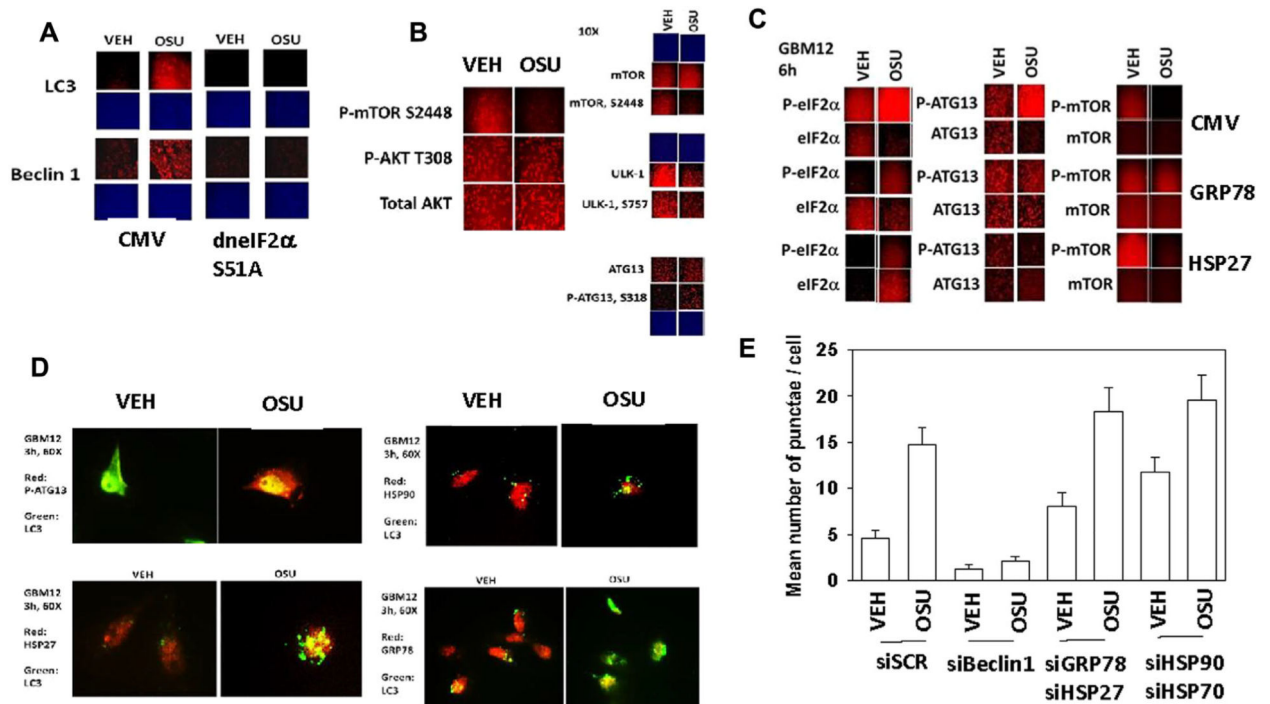
**Fig. 3.**

OSU-03012 reduces the expression of multiple chaperones and the association of chaperones with themselves and client proteins (please see Booth et al, 2016a). (A) GBM5 cells were treated with vehicle, OSU-03012 (2.0 μM) for 6 h after which cells were fixed in place and permeabilized using 0.5% Triton X100. Immuno-fluorescence was performed in the Hermes system to detect the expression level of HSP75, GRP75, BAG2, and HSP27 presented, as indicated, at 60 \times magnification. (B) GBM5 cells were treated with vehicle control or with OSU-03012 (2 μM) for 6 h after which cells were fixed in place and permeabilized using 0.5% Triton X100. Immuno-fluorescence was performed to detect the co-localization of HSP70 and BAG2; and to detect the co-localization of HSP90 and Aha1 presented at 60 \times magnification. (C) GBM5 cells were treated with vehicle control or with AR-12 (OSU-03012) (1 μM) for 3 h. Cells were fixed in place and permeabilized using 0.5% Triton X100. Immuno-fluorescence was performed to detect the expression of the indicated chaperones pair-wise. Images were merged in Adobe Photoshop to indicate areas of co-localization (red + green = yellow). (D) Upper: HeLa cells were pre-treated for 20 min with vehicle control (DMSO) or 5 μM OSU-03012 then lysed, and clarified lysates subjected to gel filtration on a Superdex column in the presence of the drug. Fractions of 1.0 ml were taken (15 fractions) and the protein precipitated from the fractions on ice using 10% (w/v) trichloro-acetic acid. Recovered protein was washed with cold 100% acetone. The protein pellets were boiled in SDS PAGE sample buffer containing bromophenol blue and subjected to SDS PAGE on 12% acrylamide gels, followed by western blotting to determine the elution profiles of HSP27. Lower: GBM12 cells were treated with vehicle or with OSU-03012 (2 μM) for 10 min and then lysed. Immuno-precipitation of HSP90, GRP78, HSP27, and HSP70 was performed in the presence or absence of drug (2 μM) for 3 h. Cells were washed with lysis buffer in the presence or absence of drug individually (3 \times 1 h, each). Immuno-precipitates were then boiled in SDS PAGE buffer containing glycerol and bromo-

phenol blue. Proteins were separated on SDS PAGE (12% and 14% gels) and immunoblotting performed for the proteins as indicated. E: GBM12 cells were transfected with a plasmid to express HSP70-GFP or to express FLAG-tagged HSP90. Twenty-four hours after transfection chaperone proteins were immuno-precipitated using their tags. Equal portions of precipitate sepharose beads were immediately aliquoted into individual wells in a 96 well plate. Beads were resuspended in ATPase reaction buffer containing vehicle control; OSU-03012; sorafenib tosylate; pazopanib (30 nM; 100 nM; 300 nM; 1 μ M) in triplicate, and incubated for 30 min at 37 °C. The reaction was started by addition of ATP-lite substrate. The plate was removed from the incubator and placed into a Vector 3 plate reader to determine the luminescence of the reactions under each treatment condition ($n = 3 (x3) \pm$ SEM).

**Fig. 4.**

OSU-03012 suppresses expression of glucosidase I, glucosidase II α and calnexin via inhibition of GRP78 and HSP27 function. A: HuH7 and HT1080 cells were treated with vehicle, OSU-03012 (0–3 μ M), sildenafil (2 μ M) or the drugs in combination. Two hours after drug exposure cells were fixed in place and permeabilized. Immuno-fluorescence was performed to determine the total cellular levels of TIM1 and NPC1 (Ebola/Marburg virus receptors) ($n = 3 \pm$ SEM). B: HuH7 cells were transfected with an empty vector plasmid or plasmids to express GRP78 and HSP27 together. Twenty-four hours after transfection cells were treated with vehicle control or with OSU-03012 (2.0 μ M) \pm sildenafil (2 μ M) for 6 h after which cells were fixed in place and permeabilized using 0.5% Triton X100. Immuno-fluorescence was performed to detect the expression of NPC1 at 10 \times using a Hermes WiScan system. C: GBM12 cells were treated with vehicle, OSU-03012 (2.0 μ M) for 6 h after which cells were fixed in place and permeabilized using 0.5% Triton X100. Immuno-fluorescence was performed to detect the expression levels of glucosidase I; glucosidase II α ; and glucosidase II β at 10 \times magnification using a Hermes WiScan system. D: ADOR lung cancer cells (a July 2015 PDX model) were transfected with an empty vector plasmid or plasmids to express GRP78 and HSP27 together. Twenty-four hours after transfection cells were treated with vehicle control or with OSU-03012 (2.0 μ M) \pm sildenafil (2 μ M) for 6 h after which cells were fixed in place and permeabilized using 0.5% Triton X100. Immuno-fluorescence was performed to detect the expression levels of Calnexin; glucosidase I; and glucosidase II α at 10 \times magnification using a Hermes WiScan system.

**Fig. 5.**

OSU-03012, via inhibition of GRP78 and HSP27, facilitates an eIF2 α -dependent increase in Beclin1 and LC3 expression in parallel with mTOR inactivation and ATG13 phosphorylation leading to autophagosome formation. **A:** GBM5 cells were transfected with either an empty vector plasmid (CMV) or a plasmid to express dominant negative eIF2 α S51A. Twenty-four hours after transfection cells were treated with vehicle, OSU-03012 (2.0 μ M) for 6 h after which cells were fixed in place and permeabilized using 0.5% Triton X100. Immuno-fluorescence was performed to detect the expression levels of LC3 (ATG8) and Beclin 1 (ATG6). **B:** GBM5 cells were treated with vehicle, OSU-03012 (2.0 μ M) for 6 h after which cells were fixed in place and permeabilized using 0.5% Triton X100. Immuno-fluorescence was performed to detect the total expression levels of AKT/ULK-1/ATG13/ mTOR, and the phosphorylation levels of AKT T308; mTOR S2448; ULK-1 S757; ATG13 S318. **C:** GBM12 cells were transfected with empty vector (CMV), or plasmids to express GRP78 or HSP27. Twenty-four hours after transfection cells were treated with vehicle, OSU-03012 (2.0 μ M) for 6 h after which cells were fixed in place and permeabilized using 0.5% Triton X100. Immuno-fluorescence was performed to detect the total expression levels of mTOR; eIF2 α and ATG13 as well as the phosphorylation of mTOR S2448; eIF2 α S51; ATG13 S318, presented at 10 \times magnification. **D:** GBM12 cells were treated with vehicle, OSU-03012 (2.0 μ M) for 3 h. Cells were fixed in place and permeabilized using 0.5% Triton X100. Immuno-fluorescence was performed at 60 \times magnification to detect the co-localization of HSP27 with LC3 and of phospho-ATG 13 S318 and LC3. GBM 12 cells were treated with vehicle, OSU-03012 (2.0 μ M) for 3 h. Cells were fixed in place and permeabilized using 0.5% Triton X100. Immuno-fluorescence was performed at 60 \times magnification to detect the co-localization of GRP78 with LC3 and of HSP90 and LC3. **E:** GBM12 cells were transfected with a plasmid to express LC3-GFP and in parallel

transfected with scrambled siRNA (siSCR) or siRNA molecules to knockdown: Beclin1; (GRP78 + HSP27); (HSP90 + HSP70). Twenty-four hours after transfection cells were treated with vehicle control or were treated with OSU-03012 (2 μ M) for 6 h. Living cells were images in a Hermes Wiscan microscope at 60X magnification and the mean number of high intensity GFP+ punctae per cell determined (n = 3 \pm SEM, with >40 cells per treatment per repeated included).

Author Manuscript

Author Manuscript

Author Manuscript

Author Manuscript

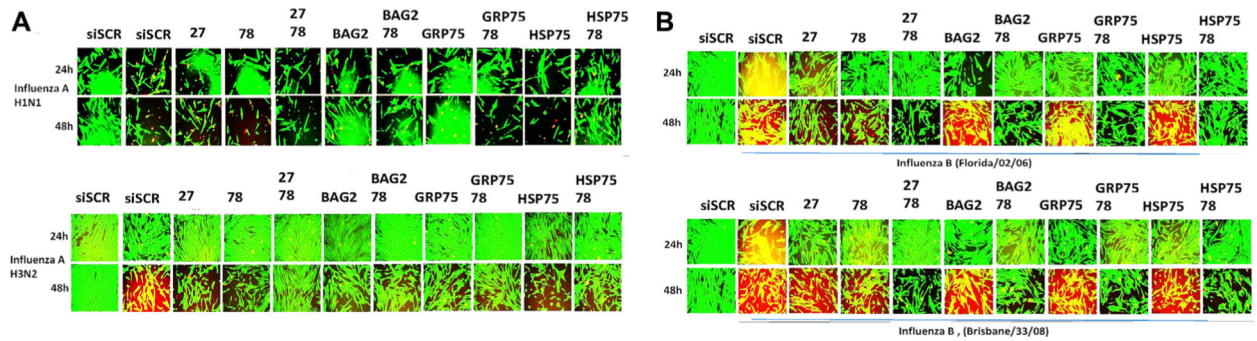
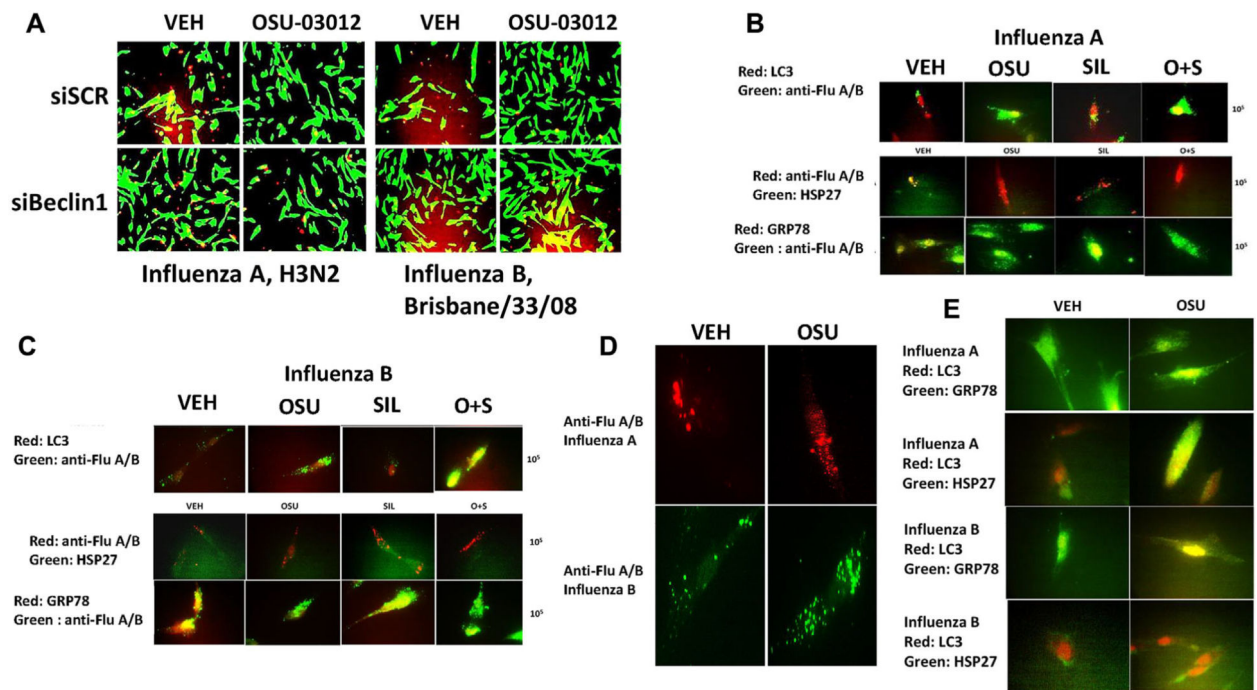
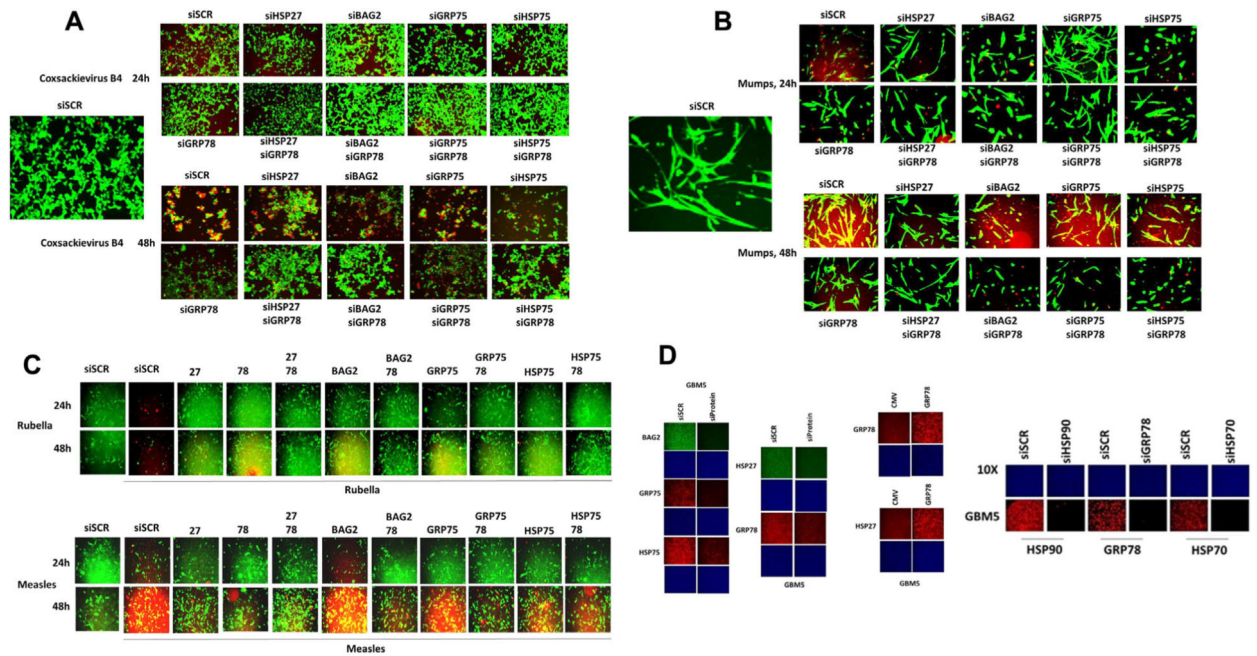


Fig. 6.

Knock down of GRP78 and HSP27 suppresses influenza virus replication. A: MRC5 cells were transfected with a scrambled siRNA (siSCR) or siRNA molecules to knock down the expression of HSP27, BAG2, GRP75, HSP75, and GRP78. Twenty-four hours after transfection cells were infected with Influenza A viruses (1,000 particles per cell). Cell viability was determined 24 and 48 h after virus infection. B: MRC5 cells were transfected with a scrambled siRNA (siSCR) or siRNA molecules to knock down the expression of HSP27, BAG2, GRP75, HSP75, and GRP78. Twenty-four hours after transfection cells were infected with Influenza B viruses (1,000 particles per cell). Cell viability was determined 24 and 48 h after virus infection.

**Fig. 7.**

OSU-03012 suppresses influenza virus replication, in part, by modulating chaperone function and autophagy. **A:** MRC5 cells were transfected with a scrambled siRNA (siSCR) or an siRNA to knock down Beclin 1 expression. Twenty-four hours after transfection cells were infected with Influenza viruses, as indicated (1,000 particles per cell). One hour after infection cells were treated with OSU-03012 (2 μ M) for 12 h, after which cells were washed and grown in drug free media. Cell viability was determined 24 h after virus infection. **B-E:** MRC5 cells were infected with influenza viruses (A or B) and 12 h after infection treated for 3 h with vehicle control, OSU-03012 (2 μ M), sildenafil (2 μ M), or both drugs together. Cells were fixed in place and permeabilized using 0.5% Triton X100. Immuno-fluorescence was performed to detect the co-expression/association of: LC3 and HSP27; LC3 and GRP78; LC3 and the anti-influenza antibody M149; GRP78 and the anti-influenza antibody M149; HSP27 and the anti-influenza antibody M149.

**Fig. 8.**

Modulation of viral reproduction in vitro by HSP27 and GRP78. A: HEK293 cells were transfected with a scrambled siRNA (siSCR) or siRNA molecules to knock down the expression of HSP27, BAG2, GRP75, HSP75, and GRP78. Twenty-four hours after transfection cells were infected with Coxsackievirus B4 (1,000 particles per cell). Cell viability was determined 24 and 48 h after virus infection. B: MRC5 cells were transfected with a scrambled siRNA (siSCR) or siRNA molecules to knock down the expression of HSP27, BAG2, GRP75, HSP75, and GRP78. Twenty-four hours after transfection cells were infected with Mumps (1,000 particles per cell). Cell viability was determined 24 and 48 h after virus infection. C: MRC5 cells were transfected with a scrambled siRNA (siSCR) or siRNA molecules to knock down the expression of HSP27, BAG2, GRP75, HSP75, and GRP78. Twenty-four hours after transfection cells were infected with Measles virus or Rubella virus (1,000 particles per cell, each). Cell viability was determined 24 h and 48 h after virus infection. D: Control siRNA immunofluorescence images are presented showing the knock down of various proteins. Cells were transfected with a scrambled siRNA or an siRNA to knock down a particular protein. Twenty-four hours after transfection the cells are fixed and stained. Immunofluorescence is examined at 10× magnification in the Hermes wide-field microscope.

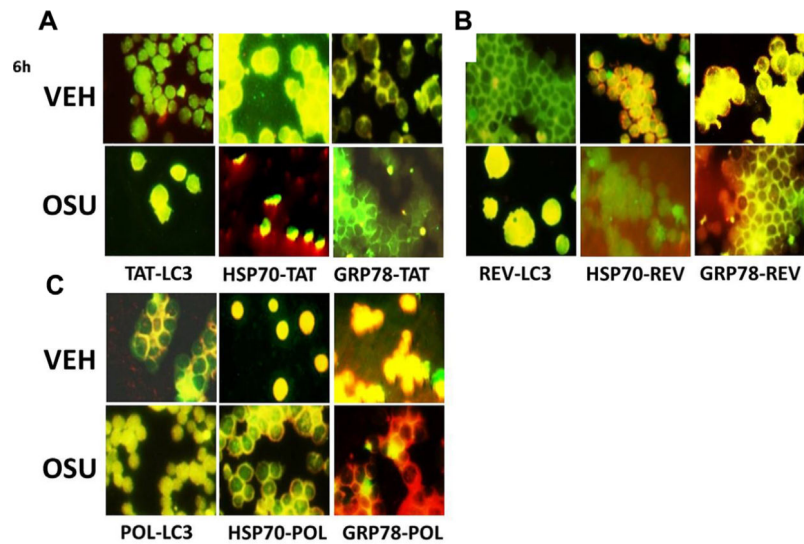
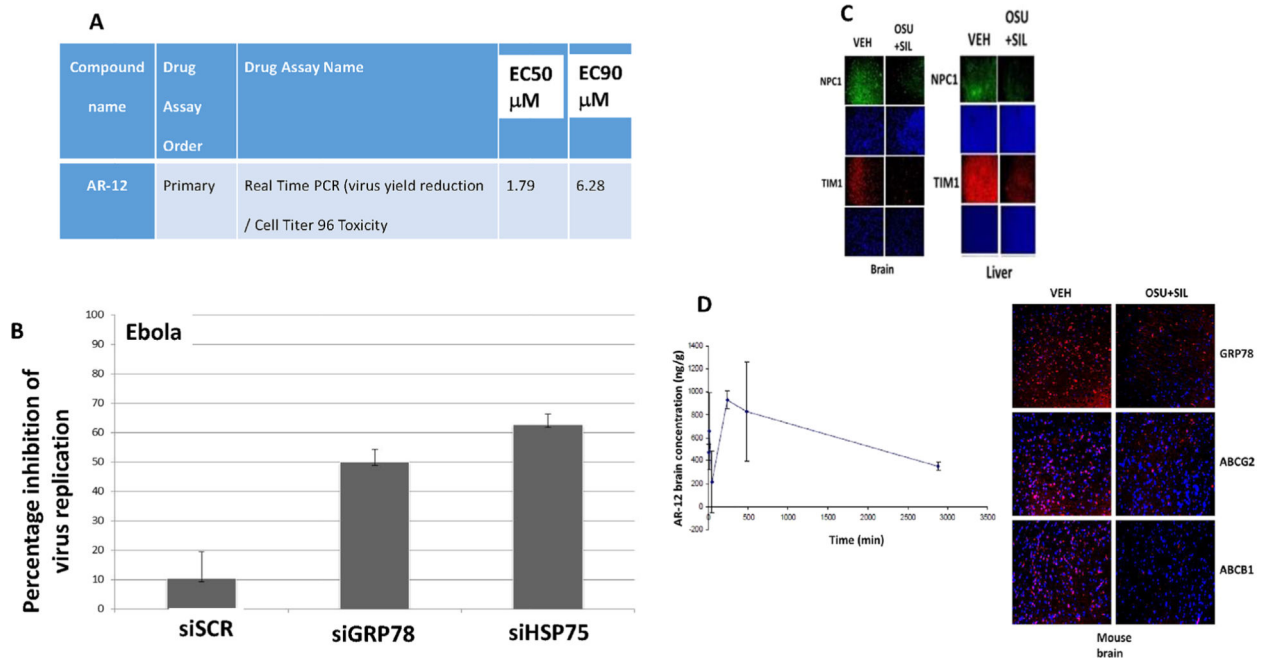
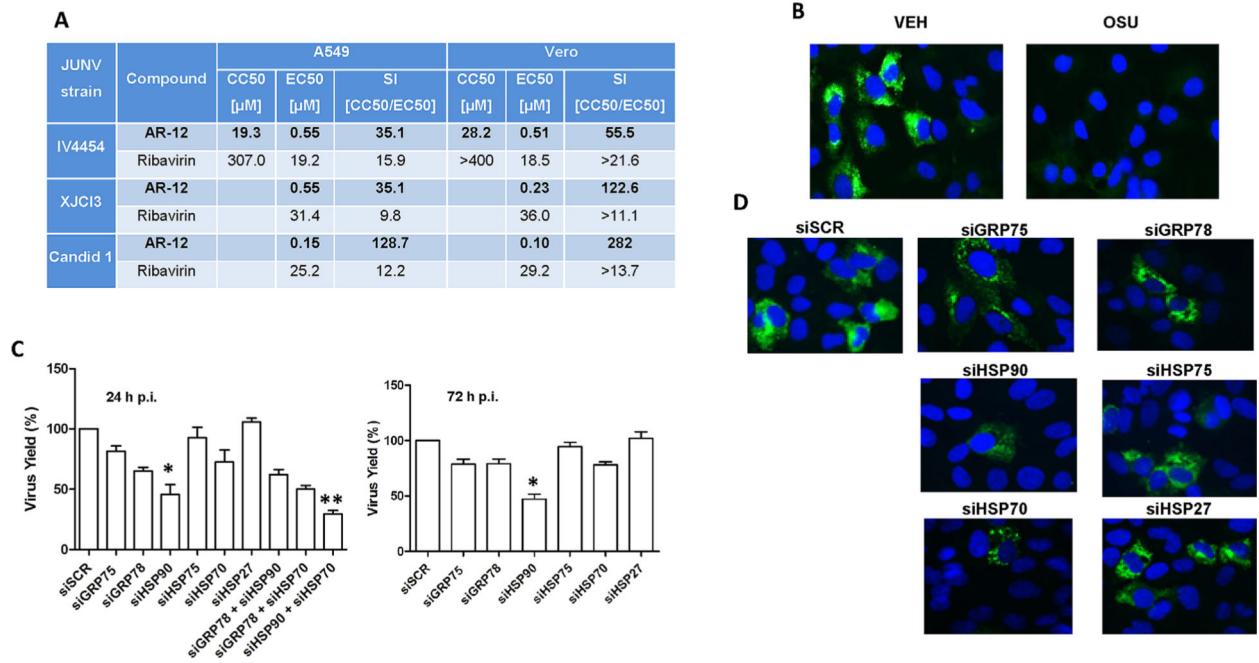


Fig. 9.

OSU-03012 suppresses HIV replication, in part, by modulating chaperone function and autophagy. A-C: RAW264.7 mouse macrophage cells were transfected with a plasmid to express the HIV proteins Gag-Pol, Tat and Rev; and 24 h after transfection treated for 6 h with vehicle control or OSU-03012 (2 μ M). Cells were fixed in place and permeabilized using 0.5% Triton X100. Immuno-fluorescence was performed to detect the co-expression/association of: LC3 and the HIV proteins Gag-Pol, Tat, Rev; GRP78 and the HIV proteins Gag-Pol, Tat, Rev; HSP70 and HIV proteins Gag-Pol, Tat, Rev at 10 \times magnification in the Hermes wide-field microscope.

**Fig. 10.**

OSU-03012 suppresses the reproduction of Ebola virus. **A:** Near confluent HEK293T reporter cells (enzyme-linked virus reporter, ELVIRA[®]; ELVIRA Flu A-luc) were infected with Ebola virus. Cells were then treated with increasing concentrations of OSU-03012 (AR-12). Twenty-four hours after infection, cells were lysed and analyzed for firefly luciferase activity using the Bright-Glo Luciferase Assay System (Promega). The EC₅₀ and CC₅₀ values were determined for both viruses with AR12. **B:** HeLa cells were transfected with a scrambled siRNA (siSCR) or siRNA molecules to knock down the expression of HSP27, BAG2, GRP75, HSP75, and GRP78. Twenty-four hours after transfection cells were infected with Ebola virus (1,000 particles per cell). Cell viability was determined 24 and 48 h after virus infection. **C:** Mice were co-administered IP, OSU-03012 (50 mg/kg) and sildenafil (10 mg/kg) for 5 days after which time animals were humanely sacrificed and the brains and livers of animals isolated, fixed in formaldehyde, and embedded in paraffin wax. Ten micron sections of tissue were taken, de-parafinized and renatured, and immunohistochemistry performed to detect the expression of TIM1 and NPC1. **D:** Mice were administered OSU-03012 (10 mg/kg) as a bolus IV. Animal brains were isolated after drug treatment at the indicated time points, and the concentration of OSU-03012 in the mouse brain determined (ng/g \pm SEM; OSU-03012 molecular weight of 460.45).

**Fig. 11.**

OSU-03012 (AR-12) is a potent inhibitor of JUNV replication. A: A549 and Vero cells were mock-infected or infected with different JUNV strains (multiplicity 1 PFU/cell). Cells were then treated with increasing concentrations of OSU-03012 (AR-12) or ribavirin. At 48 h after infection cell viability was determined in mock-infected cells by MTT method and virus yields were measured in infected cells by PFU. Cytotoxic concentration 50% (CC₅₀) and effective concentration 50% (EC₅₀) were then extrapolated from dose-response curves. B: In A549 cells infected with JUNV IV4454 and treated with vehicle or 1.25 m-M OSU-03012 (AR-12), viral nucleoprotein NP was determined by indirect immunofluorescence with mAb SA02-BG12 at 48 h after infection (600 \times magnification). C: A549 cells were transfected with a scrambled siRNA (siSCR) or siRNA molecules to knock down the expression of HSP27, HSP70, HSP75, HSP90, GRP75, and GRP78. Twenty-four hours after transfection cells were infected with JUNV (1 PFU/cell) and virus infectivity was determined by PFU at 24 or 72 h after virus infection. Results are expressed as % virus yield related to siSCR treated cells \pm SD * $P < 0.05$ less than scrambled control; ** $P < 0.05$ less than siHSP90 alone value. D: In A549 cells transfected with siRNAs and infected with JUNV as in *Panel C*, viral nucleoprotein (NP) was determined by indirect immunofluorescence with mAb SA02-BG12 24 h after infection (600 \times magnification).

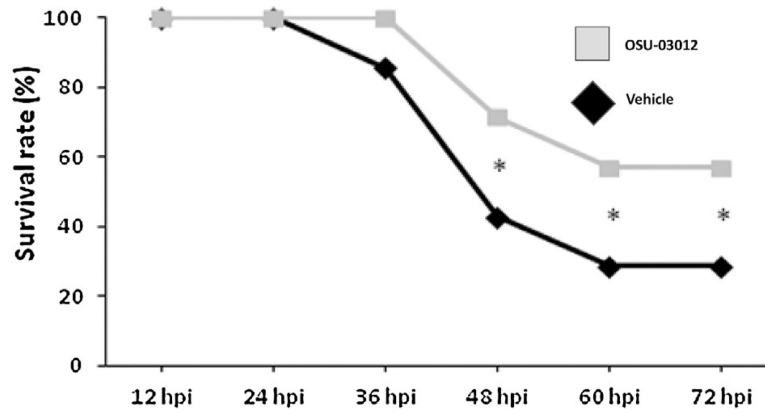


Fig. 12.

Effects of OSU-03012 (AR-12) on survival rates after RHDV infection. Nine-week-old New Zealand white rabbits were kept in the animal facility of the University of León. The rabbits were kept in a climatized room at 21°C, with a 12 h light cycle. They were given a standard dry rabbit food and water ad libitum. For animal survival studies, 14 animals were injected intramuscularly with 2×10^4 hemagglutination units of RHDV isolate Ast/89. Seven were treated with vehicle control and seven with OSU-03012 (25mg/kg) at 0, 12, 24, and 36 h post infection. Animal survival was monitored twice daily. Data represent percentage of surviving animals. * $P < 0.05$ with Fisher test.

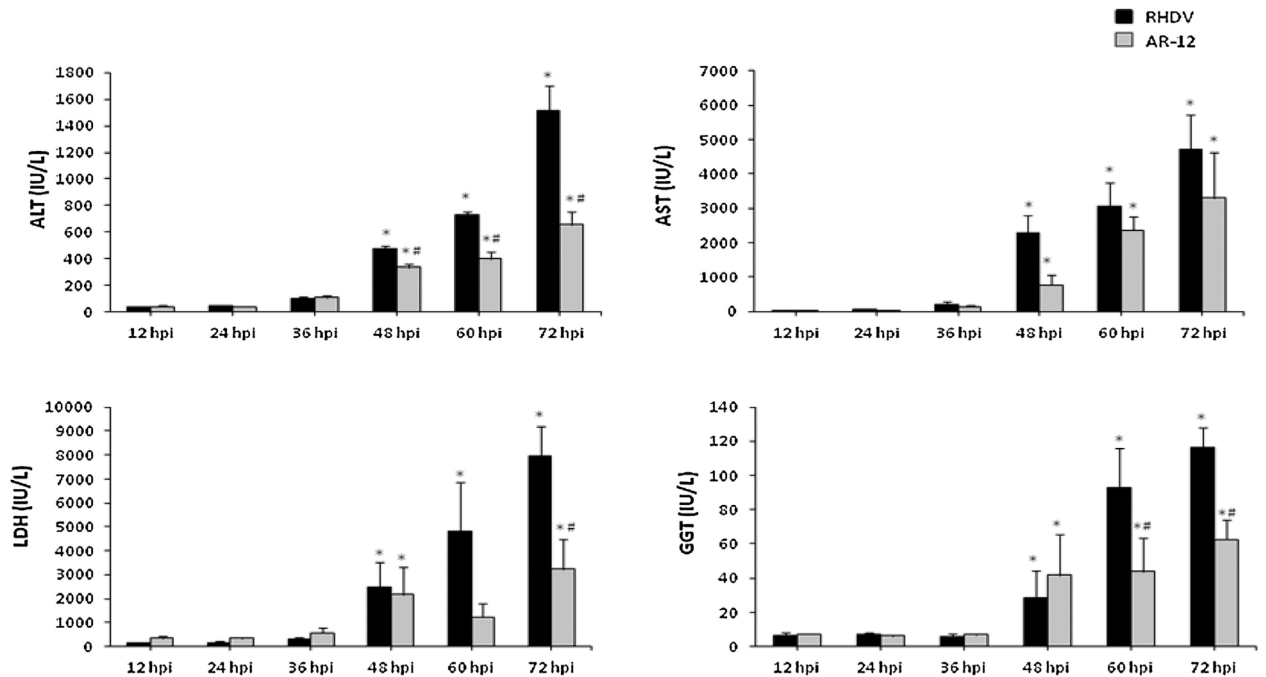


Fig. 13.

Effect of RHDV-infection and OSU-03012 (AR-12) treatment on rabbit blood biochemistry. Nine-week-old New Zealand white rabbits were kept in the animal facility of the University of León. The rabbits were kept in a climatized room at 21°C, with a 12 h light cycle. They were given a standard dry rabbit food and water ad libitum. For animal survival studies, 14 animals were injected intramuscularly with 2×10^4 hemagglutination units of RHDV isolate Ast/89. Seven were treated with vehicle control and seven with OSU-03012 (25 mg/kg) at 0, 12, 24, and 36 h post infection. Plasma was obtained at the indicated time points and the levels of alanine aminotransferase (ALT), aspartate aminotransferase (AST), lactate dehydrogenase (LDH), and gamma-glutamyl transferase (GGT) determined for all viable animals. * $P < 0.05$ compared with 12hpi. # $P < 0.05$ compared with RHDV.

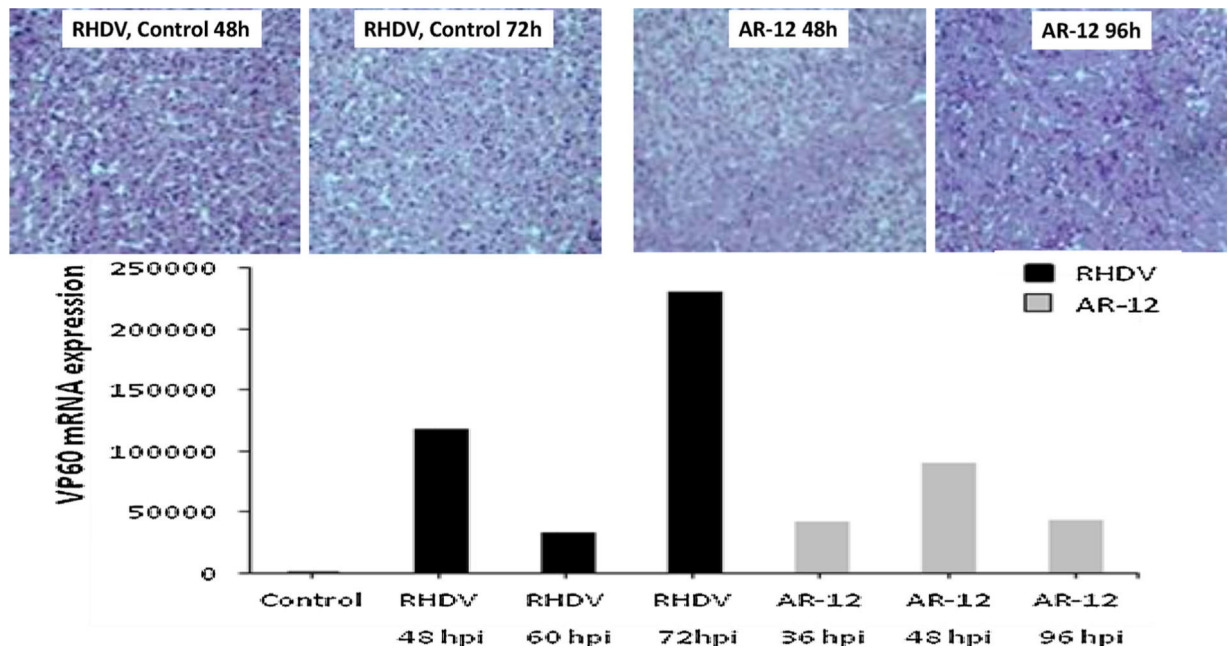


Fig. 14.

OSU-03012 (AR-12) suppresses the production of VP60 capsid protein mRNA that correlates with reduced liver damage as judged by H&E staining. Nine-week-old New Zealand white rabbits were kept in the animal facility of the University of León. The rabbits were kept in a climatized room at 21°C, with a 12 h light cycle. They were given a standard dry rabbit food and water ad libitum. For animal survival studies, 14 animals were injected intramuscularly with 2×10^4 hemagglutination units of RHDV isolate Ast/89. Seven were treated with vehicle control and seven with OSU-03012 (25 mg/kg) at 0, 12, 24, and 36 h post infection. At the time of animal death, the livers were removed. Upper images: portions of the livers were fixed, 10 micron sections taken, and stained with H&E before histologic imaging at 10× magnification; Lower Graph: portions of the livers were processed to isolate total mRNA and the levels of VP60 mRNA determined by quantitative RT-PCR.

TABLE 1.

OSU-03012 (AR-12) is a potent inhibitor of HIV replication

Test article	HIV isolate	High testconcentration	IC50 (µM)	TC50 (µM)	Antiviral index (TC50/IC50)
AR-12	HIV-191US001	30 µM	0.24	6.12	25.6
	HIV-1 92HT599		0.27		22.6
	HIV-2 CBL20 H9		0.51		12.0
	HIV-2 CDC 310319		0.37		16.4
AZT	HIV-MDR 769		0.310		19.9
	HIV-1 91US001	1,000 nM	17.4	>1,000	>57.5
	HIV-1 92HT599		11.9		>84.0
	HIV-2 CBL20 H9		<0.1		>10,000
	HIV-2 CDC 310319		5.73		>174
	HIV-MDR 769		>1,000		NA
Efavirenz	HIV-MDR 769	1,000 nM	0.66	>1,000	>1,506
Lopinavir	HIV-MDR 769	1,000 nM	827	>1,000	>1.21

Human PBMCs were infected with various HIV strains in the presence or absence of the indicated drugs, as described in Methods. Quantitative RT-PCR for the levels of reverse transcriptase mRNA. Using an in-house computer program, the PBMC data analysis includes the calculation of IC50 (50% inhibition of virus replication), IC95 (95% inhibition of virus replication), and therapeutic index values (TI = TC/IC; also referred to as Antiviral Index or AI). These studies were performed under DAIDS/NIAID contract N01-AI-14000101; Roger Miller, Project Officer.

OSU-03012 (AR-12) suppresses the replication of multiple protease inhibitor resistant strains of HIV1

TABLE 2.

HIV-1 Isolate	Compound ID	IC ₉₀ (nM)	IC ₅₀ (nM)	tc ₅₀ (nM)	TI (TC ₅₀ /TC ₉₀)
NL4-3	AR-12	2,169	749	5,532	7.39
	AZT	39.6	9.96	>1,000	>100
	Ritonavir	92.3	45.5	>10,000	>220
	Raltegravir	5.18	1.30	>100	>77.0
	Nevirapine	227	75.3	>10,000	>133
MDR769	Delavirdine	57.6	30.6	>2,000	>65.5
	T-20	412	133	>2,000	>15.0
	Elvitegravir	1.25	0.52	>1,000	>1,935
	AR-12	3,819	848	5,532	6.53
	AZT	>1,000	>1,000	>1,000	N/A
MDR807	Ritonavir	>10,000	>10,000	>10,000	N/A
	Raltegravir	8.95	3.64	>100	>27.4
	AR-12	2,126	905	5,532	6.12
	AZT	>1,000	162	>1,000	>6.17
	Ritonavir	5,938	1,281	>10,000	>7.81
A17	Raltegravir	2.16	0.46	>100	>219
	AR-12	6,637	914	5,532	6.05
	AZT	27.4	11.6	>1,000	>86.0
	Nevirapine	>10,000	>10,000	>10,000	N/A
	Delavirdine	>2,000	>2,000	>2,000	N/A
1022-48	AR-12	3,679	489	5,532	11.3
	AZT	>1,000	>1,000	>1,000	N/A
	Nevirapine	242	70.4	>10,000	>142
	Ritonavir	>10,000	>10,000	>10,000	N/A
	AR-12	2,245	762	5,532	7.26
4736_4	AZT	20.6	2.57	>1,000	>389
	Raltegravir	>100	74.5	>100	>1.34
	Elvitegravir	251	81.9	>1,000	>12.2

Author Manuscript

Author Manuscript

Author Manuscript

Author Manuscript

HIV-1 Isolate	Compound ID	IC ₉₀ (nM)	IC ₅₀ (nM)	tc ₅₀ (nM)	TI (TC ₅₀ /TC ₉₀)
NL4-3 gp41 (36G) N42T, N43K	AR-12	7,372	1,016	5,532	5.45
	AZT	40.3	11.1	>1,000	>90.1
	T-20	1,773	646	>2,000	>3.10

Human PBMCs were infected with various HIV strains in the presence or absence of the indicated drugs, as described in Methods. Quantitative RT-PCR for the levels of reverse transcriptase mRNA. Using an in-house computer program, the PBMC data analysis includes the calculation of IC₅₀ (50% inhibition of virus replication), IC₉₀ (90% inhibition of virus replication), IC₉₅ (95% inhibition of virus replication), and therapeutic index values (TI = TC/IC; also referred to as Antiviral Index or AI). These studies were performed under DAIDS/NIAID contract N01-AI-14000101; Roger Müller, Project Officer.